UNIVERSIDADE DE LISBOA
FACULDADE DE CIÊNCIAS
BIOLOGIA VEGETAL

Oligometastatic Prostate Cancer: Characterization of its Molecular Phenotype

Sara Trindade Correia

Mestrado em Biologia Molecular e Genética

Dissertação orientada por:
Doutora Mireia Castillo-Martin
Professora Doutora Rita Maria Pulido Garcia Zilhão

2017

Acknowledgements

I would like to express my special thanks of gratitude to my supervisor Mireia Castillo-Martin who gave me the golden opportunity to do this research project on Prostate Cancer, and to Javier Martin, who taught me how to work with the multispectral microscope, as well as the importance of always having SOPs around. Many thanks to my co-supervisor Rita Zilhão, and my colleague and friend Andreia Maia, who gave me the strength and motivation needed when things got a bit difficult.

Secondly, it's mandatory to thank the amazing Costa-Silva lab, explicitly the P.I Bruno Costa-Silva, who kindly helped us in the early days with laboratory material and supplies. And to the incredible girls that work in this lab: Inês Ferreira, Joana Maia and Bruna Ferreira, that always took a minute to answer all my naïve questions and doubts, and never minded me running along their experiments, teaching me "how to do science": I cannot thank you enough.

Furthermore, I would also like to acknowledge with much appreciation the crucial role of the staff of the department of Anatomy and Histology at the Champalimaud Foundation, giving a special thanks to the laboratory technician Leo Madruga, who helped me greatly by processing all my cases.

Thanks to all my Master colleagues, with whom I shared wonderful moments, for giving me true friendships and a real sense of belonging in a group of students. Bárbara Correia, my ultimate sister, thanks for a great friendship. With our method of mutual motivation and senseless complimenting, nothing can bring us down. I would also like to thank a special duo of friends, my partners in crime/science, namely Ana Rosa Abreu and Bárbara Gomes, who were present every day, and together we managed to get through, using inspirational speeches and daily humour. Diana Reis, one of the strongest people I've ever met in my life, you were always on my mind. Continue strong, tackling the world with your great humour and confidence.

To all the amazing people I've met during this journey at CCU, all the labs, from exosomes and cancer research, cell fitness to zebrafish group behaviour, and to computational neurosciences, thank you so much for all your kindness, welcoming and educating me on how to party like true scientists. You convinced me that making friends can be an ageless process. Cat and Benny, with you it was easy to joke, you can always count on me for conversations about our future perspectives and motivational speeches.

Last but not least, I must thank all my family, specially my parents, my sister and closest friends. A special thanks to my uncle João, who kindly and quickly converted all my scanned images to the cmyk color scheme. To my mother: Thank you so much for showing me the strongest version of you in the most difficult times, for teaching me that life goes on whether you feel ready or not, and that all opportunities to grow professionally and personally must be seized and fully experienced.

Resumo

O Cancro da Próstata (CaP) é o tipo de cancro mais comum a afetar os homens. Tem uma incidência de 22,8% na Europa, e é o terceiro cancro responsável por mais mortes, ultrapassado pelo cancro do pulmão e do colon. Os CaP são, na grande maioria, adenocarcinomas, e têm origem nas células luminais das glândulas prostáticas. Estes tumores são caracterizados pela proliferação de células que se assemelham, tanto em estrutura como em bioquímica, com as células luminais, e pela ausência de células basais, sendo que estas últimas são as células que fazem a barreira entre as glândulas e o estroma na próstata normal. Ainda não há certezas sobre quais são as causas deste tipo de cancro, mas o aumento da idade, etnicidade e hereditariedade são fatores de risco já identificados.

A partir de uma coorte de 29 pacientes com Cancro da Próstata Oligometastático (CaP-OM), obtivemos onze amostras de tecido de oito doentes, conservadas em blocos de parafina. Estas amostras foram analisadas e comparadas, após a realização de um protocolo de imunofluorescência com cinco biomarcadores (5-plex), que nos possibilitou observar a expressão de múltiplas proteínas numa única imagem. O estado oligometastático (OM) designa que o doente tem um número limitado de lesões metastáticas (entre três a cinco metástases, mas apenas até três nestes doentes), e aparenta ser um estado intermédio entre cancro da próstata confinado ao órgão, e um estado polimetástatico (PM), de doença já disseminada pelo corpo, onde a probabilidade de sobrevivência é muito baixa. Um estudo realizado pelo Dr. Carlo Greco na Fundação Champalimaud permitiu observar que alguns doentes com CaP-OM, cujas metástases foram tratadas com Radioterapia de dose única (SDRT de 'Single Dose Radiotherapy'), normalmente 24Gy numa única sessão, responderam melhor ao tratamento, e ficaram num estado de doença controlado. A existência de uma estratificação entre doentes com CaP-OM que respondiam, ou não, ao tratamento com SDRT levou a sugerir que existiria um verdadeiro estado OM, o qual apresentaria uma biologia tumoral característica, ainda potencialmente curável.

Há cada vez mais uma necessidade de encontrar novos biomarcadores que possam auxiliar o diagnóstico clínico de doentes com CaP, colaborando com o tão conhecido exame do nível de PSA (antigénio específico da próstata) sanguíneo que, até aos dias de hoje, continua a ser a principal ferramenta utilizada no diagnóstico e seguimento dos doentes. No entanto, este exame tem sido alvo de muitas controvérsias, pois apresenta uma especificidade baixa, tal devido ao facto de algumas condições benignas poderem levar a elevações no nível desta proteína e, consequentemente, a falsos diagnósticos e a tratamentos excessivos e desnecessários.

O protocolo de coloração utilizado neste estudo foi adaptado de um protocolo criado e otimizado no Centro Hospitalar Mount Sinai, em Nova Iorque. Este protocolo continha cinco anticorpos todos com interesse na identificação e caracterização dos CaP. Estes anticorpos permitiram fazer uma definição do tecido e rapidamente identificar estruturas normais contra tumor, possível através da utilização do anticorpo para a citoqueratina 18 (CK18), uma citoqueratina de baixo peso molecular que marca células epiteliais das glândulas prostáticas, normais e tumorais. O recetor de androgénio, AR, e a racemase α-metilacil coenzima A, AMACR, já são conhecidos por terem especial interesse para a progressão do CaP, e por serem utilizados como apoio nos diagnósticos executados pelos médicos patologistas. O AR é um recetor nuclear ativado pela ligação de hormonas androgénicas, como a testosterona. Este é muitas vezes encontrado sobre-expressado nos tumores. Contudo, quer a sobre-expressão, quer o silenciamento deste gene, são ambos fenómenos relacionados com a transição para um estado independente de androgénios que, por sua vez, está relacionado com um pior prognóstico para os doentes. A AMACR é uma enzima que tem um papel importante no metabolismo dos ácidos gordos, e também se encontra muitas vezes com níveis elevados no CaP. A PSMA (antigénio membranar especifico da próstata) é uma glicoproteína transmembranar não secretada, normalmente também encontrada elevada no CaP. O Ki-67 é uma proteína nuclear que marca células em proliferação, e a percentagem de expressão desta

proteína está muitas vezes correlacionada com a progressão clínica de vários cancros, o da próstata é um deles.

Este projeto faz parte de um estudo piloto, no qual o objetivo é gerar um algoritmo inovador para o diagnóstico e seguimento da doença, utilizando dados clínicos retrospetivos, juntamente com dados fenotípicos e moleculares, permitindo fazer uma seleção de quais os doentes com CaP-OM que terão maior probabilidade de beneficiar com um certo tratamento e, consequentemente, maior probabilidade de sobrevivência. Assim, este projeto em específico tem o intuito de fazer uma descrição de alguns casos CaP-OM, abrindo caminho para uma possível caracterização do estado OM, através de diferenças encontradas entre os fenótipos moleculares nas amostras das biópsias prostáticas iniciais e das metástases, comparando também os resultados dos pacientes já falecidos com os que ainda estão vivos e a responder aos tratamentos.

No momento do diagnóstico, os oito pacientes apresentavam uma idade média de 61,9 anos e um PSA inicial médio de 11,3 ng/mL. A maior parte deles apresentava tumores no estágio TNM ("Tumor, nodes, metastasis") de T2, ou seja, tumores primários confinados na próstata.

Nesta coorte de pacientes o local mais comum de primeira metástase foi nos nódulos/órgãos linfáticos, seguidos por metástases no osso, pulmões e cérebro. O caso único de metástase na glândula adrenal constitui uma metástase atípica do CaP. O local da primeira metástase e distribuição das metástases têm mostrado ter grande impacto na prognose clínica e probabilidade de sobrevivência destes doentes. Dois destes doentes, que apresentavam semelhante diagnóstico inicial e percurso clínico de tratamento, exibiram evoluções clínicas muito diferentes, um deles falecendo por progressão cerebral. Nestes a grande diferença foi o local da primeira metástase. Aquele cuja primeira metastização foi no osso exibiu uma evolução tumoral mais rápida, não respondendo aos tratamentos, quer de terapia hormonal quer de radioterapia. A radioterapia tem um papel muito importante no controlo tumoral e na cura de todos os doentes. No entanto, e tal como podemos concluir com o grupo de doentes estudados, muitos são tratados com terapia hormonal, utilizada especialmente como primeiro tratamento, para além da cirurgia (prostatectomia radical ou parcial). O segundo tratamento, esse sim, é normalmente radioterapia, SBRT (stereotactic body radiotherapy), SDRT ou ambos.

A microscopia de fluorescência parte do principio da utilização de feixes de emissão de luz fluorescente com diferentes picos de excitação no espectro visível da luz. A microscopia multiespectral utiliza vários filtros de longa emissão que permitem a captura do sinal de emissão de mais de cinco biomarcadores diferentes, pela utilização de anticorpos marcados com *tags* fluorescentes, cujos picos de excitação e emissão são distintos, e não sobreponíveis. Após a criação de uma "biblioteca multiespectral" com os picos de emissão para todos os marcadores utilizados (AMACR, AR, CK18, Ki-67, PSMA) e DAPI, foi possível obter imagens complexas que continham uma grande quantidade de informação molecular. A análise semiautomática das imagens de amostras de cancros primários e metástases permitiu observar que as metástases apresentavam maior heterogeneidade intratumoral, com grande variação na expressão dos biomarcadores.

Três pacientes, um deles morto, permitiram fazer uma comparação dos fenótipos moleculares das amostras primárias com metástases, fazendo uma observação da progressão tumoral ao longo do tempo. Nestes doentes, as alterações examinadas entre biópsias separadas no tempo foram significativas para os marcadores PSMA e AMACR. Para além desses, o Ki-67 apresentou sempre um aumento de expressão estatisticamente significativa, revelando o potencial deste biomarcador como indicador de progressão tumoral.

A análise de sobrevivência, pelas curvas Kaplan-Meier, apresentou resultados interessantes pois observámos que doentes apresentaram níveis baixos de marcadores como AR e Ki-67 exibiram maior probabilidade de sobrevivência.

A análise de todas as amostras possibilitou a identificação de um possível fenótipo ao qual corresponde maior agressividade tumoral, associado a um pior cenário clínico e a uma maior

probabilidade de recorrência tumoral. Este corresponde a uma elevada expressão do AR, Ki-67 e possivelmente também dos marcadores AMACR e PSMA, embora estes apresentem uma expressão mais variada entre os pacientes. A perda de expressão de biomarcadores como AR e PSMA, também mostrou ser um sinal de progressão, observado nalguns pacientes com pior prognóstico. Todos os pacientes que apresentaram o Ki-67 sobre-expressado, com valores acima dos 20%, não responderam aos tratamentos e acabaram por morrer da doença. Tal insinua que este marcador poderá ter elevada importância como ferramenta para gestão clínica de pacientes num estado mais avançado da doença, assim como para previsão da progressão tumoral e resposta aos tratamentos, nomeadamente RT.

Palavras-chave: Cancro da Próstata, Oligometástases, Imunofluorescência, Microscopia multiespectral, Biomarcadores

Abstract

Prostate Cancer (PCa) is the most common malignancy affecting men. PCa is a clinically heterogeneous disease, both histologically and clinically, what implies variability in patient outcomes. Novel biomarkers for outcome prediction are urgently needed aiding the postoperative monitoring of high-risk patients. Our working hypothesis contemplates that Oligometastatic PCa (OM-PCa) represents a potentially curable early metastatic phase. This project included eight OM-PCa retrospective consented patients who received radiotherapy (RT) treatment at the Champalimaud Clinical Centre, for whose we got eleven tissue samples in FFPE blocks corresponding to primary tumor and metastasis. Using a multiplex immunofluorescence (IF) assay and multispectral microscopy we analysed the expression of multiple biomarkers (CK18, AR, AMACR, PSMA, and Ki-67) and DAPI as a counterstain in a single image, quantifying the expression levels in a semi-automated way using an open image analysis software.

This project aimed to generate a novel diagnostic algorithm for OM-PCa using retrospective clinical data, molecular and phenotypic signatures of tissue samples, eventually enabling the stratification of patients per individual risk, possible phenotypic signatures and tumor response to treatments.

The eight patients presented a mean age and PSA at diagnosis of 61,9 years, and 11,3 ng/mL, respectively. After the initial diagnosis, the great majority of the patients underwent hormone therapy (HT) or surgery (radical prostatectomy – RP). The most common second and third treatments, corresponded to RT, either SBRT (stereotactic body radiotherapy) or SDRT (single dose radiotherapy). Out of the eight patients, three died of the disease with a mean follow-up of 111,6 months, and another three, for whose we had more than one tissue sample available, allowed the analysis of changes in the tumor phenotype with time. The potential of the multiplex IF technique in research is vast, since it allows the visualization and quantification of multiple biomarkers that are spatially distributed along the tissue and co-expressed at the sub-cellular level. The comparison between the molecular phenotypes of the primary PCa and metastatic samples showed that the later tissues presented greater biomarkers expression variability amongst patients. Ki-67 showed an interesting and statistically significant increase in time, being overexpressed in all analysed metastatic tissues, suggesting that this marker may be associated with tumor progression and the acquisition of a more aggressive phenotype. The impact of the metastasis site in the patient's prognosis and probability of survival has received growing importance, showing that patients whose first metastatic site is the bone present higher probability of recurrence and tumor progression, which was observed in this group of patients.

In conclusion, a possible aggressive molecular phenotype, associated with a worse disease scenario and shorter recurrent-free survival, would present high expression of AR, Ki-67 and possibly overexpression of AMACR and PSMA, although these latter are very heterogeneously expressed along metastatic samples.

Key-words: Prostate Cancer, Oligometastasis, Immunofluorescence, Multispectral microscopy, Biomarkers

List of Figures

List of Tables

List of Acronyms

ADT Androgen-deprivation therapy
AMACR α-methylacyl coenzyme A racemase
AR Androgen receptor
AR-V7 AR splice variant 7
BM Bone metastasis
BPH Benign prostatic hyperplasia
cfDNA Cell-free DNA
CK18 Cytokeratin 18
CK5/6 Cytokeratin 5/6
CRPC Castrate-resistant prostate cancer
CSC Cancer stem cell
CT Computed tomography
CTCs Circulating tumor cells
DRE Digital rectal examination
EBRT External beam radiotherapy
ERG ETS related gene
ETS erythroblast transformation-specific
FFPE Formalin-fixed paraffin-embedded
FOXA1 Forkhead box A1
GS Gleason Score
GTV Gross tumor volume
H&E Hematoxylin and eosin
HGPIN High grade prostatic intraepithelial neoplasia
HT Hormone therapy
IDH1 Isocitrate dehydrogenase 1
IF Immunofluorescence
IGRT Image-guided radiation therapy
IHC Immunohistochemistry
IMRT Intensity-modulated radiotherapy
KLK3 Kallikrein-related peptidase 3
LBD Ligand-binding domain
LDN Lymphadenectomy
LN Lymph node
nPSA Nadir PSA
OM Oligometastatic
OM-PCa Oligometastatic prostate cancer
PAP Prostatic acid phosphatase
PCa Prostate cancer
PET positron emission tomography
PM Polymetastatic
PSA Prostate-specific antigen
PSMA Prostate-specific membrane antigen
PTEN Phosphatase and tensin homolog
ROIs Regions of Interest
RP Radical prostatectomy
RT Radiation therapy/radiotherapy

SBRT Stereotactic body radiotherapy
SDRT/IG-SDRT Single dose radiotherapy/ Image-guided single dose RT
SPOP Speckle type BTB/POZ protein
SR Suprarenal
TNM tumor, nodes, metastasis classification
TP53 Tumor protein p53
TRUS Transrectal ultrasonography

Table of Contents

1 INTRODUCTION

1.1 Cancer of the prostate

Prostate cancer (PCa) is the most common malignancy affecting men in the world,[1] and it has an incidence of 22.8% in Europe.[2] This type of cancer is more frequent in men older than 60 years old and is responsible for 9.5% of cancer-related deaths in men,[2] more specifically, the lethal form of castrate-resistant prostate cancer (CRPC).[3] Differences between prevalence in geographically distant populations suggest that lifestyle and environmental risk factors can be an influence on the incidence.[4]

1.1.1 The prostate gland

The prostate gland is an exocrine gland and one of the male reproductive accessory glands, with an important role in male fertility, which relies on the composition of the secreted prostatic fluid. This gland can be affected by several benign and malignant diseases that can be a threat to male fertility and normal urinary function.[5]

1.1.2 Characterization of adenocarcinomas of the prostate and grading

Cancers of the prostate are, in the majority, adenocarcinomas,[6] mostly acinar adenocarcinomas originating in the luminal cells of prostatic glands. They are characterized by proliferation of cells that resemble luminal cells, both morphologically and phenotypically, and usually by the absence of basal cells.[7,8] However, more recent papers question if PCa can also be originated from basal cells.[9] PCa are histologically graded with the renowned Gleason grading system, which consists on the analysis of the glandular pattern and degree of differentiation, dividing them into five grades, from 1 to 5.[10,11] This grading system is considered one of the prognostic markers of PCa after being transformed into the Gleason Score, GS (sum of the two most frequent Gleason grades present in the tumor), and more recently, into five prognostic grade groups.[12]

1.1.2.1 High grade prostatic intraepithelial neoplasia and the initiation of PCa

High grade prostatic intraepithelial neoplasia (HGPIN) yields insights into the initiating events of PCa, being the most likely precursor of invasive carcinomas.[13,14] HGPIN can be found in most cases accompanying prostate adenocarcinomas, and is described by dysplasia and proliferation of the normal luminal cell layer of prostatic ducts, without invasion.[13] This architectural alteration is probably a progression event, representing an intermediate state between benign prostatic epithelium and cancer, that is evident by the manifestation of some characteristics also present in carcinomas, such as focal disruption of the basal cell layer, loss of secretory differentiation markers, nuclear and nucleolar abnormalities, increasing proliferative potential, DNA alterations and allelic loss.[15]

1.1.3 PCa, increasing age and genetic alterations

There is still no clear evidence as to what can trigger PCa, but hormonal factors are involved, and dietary habits may have an indirect effect.[16] Increasing age and ethnicity are identified risk factors of PCa,[17] and family history is another established risk factor, due to the genetic inheritance of mutations in specific PCa-related genes.[4,18] The genetic alterations found in PCa are mainly gene fusions of androgen-regulated promoters with ERG (ETS related-gene) and other members of the ETS (erythroblast transformation-specific) family of transcription factors,[19,20] losses and genetic amplifications, like the well-known overexpression of the androgen receptor (AR) gene,[21,22] suggested to emerge in response to androgen-deprivation therapy (ADT). The TMPRSS2:ERG gene fusion is the most common molecular alteration, found in 40 to 50% of PCa tumors.[23] Contrary to many solid tumors, PCa is characterized by a low frequency of somatic point mutations, being genes such as SPOP (speckle

type BTB/POZ protein), TP53 (tumor protein p53), FOXA1 (forkhead box A1), PTEN (phosphatase and tensin homolog) and IDH1 (isocitrate dehydrogenase 1, cytosolic) the most frequently mutated.[20,24] Very rare, but associated with increased risk of lethal PCa, is the inherited BCRA2 mutation, affecting the tumor suppressor gene, essential for the correct functioning of the DNA repair machinery.[25–27] Tumors of the prostate can also have variations in DNA copy-numbers. Whereas in more aggressive primary and metastatic tumors there can be found various copy-number alterations, indolent and low-Gleason nurse fewer alterations.[20,28]

1.2 Diagnosis and treatment

From a clinical point of view, PCa can be diagnosed as being local or advanced disease.[18] Around 20% of patients with local disease will experience relapse to aggressive metastatic disease in the following five to ten years,[29] being responsible for the great majority of cancer related deaths. This happens due to the high variability of localized PCa, in which, while some men have aggressive cancer that metastasizes and leads to death, many others have indolent tumors that can be cured with therapy and/or observation,[20] staying alive with or without evidence of disease.

1.2.1 PCa diagnosis and risk stratification

The management of PCa is very important, and is done by stratifying patients according to risk, differentiating between aggressive or indolent disease.[30] The D'Amico classification system, published in 1998,[31] aimed for the prediction of PCa progression, and suggested the stratification of patients into groups with a low, intermediate, or high-risk of recurrence after radical prostatectomy (RP) or radiation therapy (RT). This system was broadly accepted and it shaped the guidelines currently used in clinical management practice for PCa,[32,33] which employs an initial diagnosis based on blood serum levels of the prostate-specific antigen (PSA) protein, also known as kallikrein-related peptidase 3 (KLK3), and digital rectal examination (DRE). A transrectal ultrasonography (TRUS) is a detection method that can also be used. However, a positive prostate biopsy result, performed by a pathologist, is necessary for a definitive positive PCa diagnosis.[16,32,33] The posterior stratification into risk groups is based on the clinical TNM (tumor, nodes, metastasis) stage[34], diagnostic PSA level, biopsy GS and number of positive biopsies.[30,32,33]

1.2.2 PSA blood test as a screening and diagnosis tool

PCa diagnosis and management has long implemented a biomarker as a screening tool. Serum PSA screening has been used for over twenty years as a monitoring tool after substituting another glycoprotein specific for prostatic epithelial cells, the prostatic acid phosphatase (PAP).[35] PSA was officially approved as a screening tool by the U.S Food and Drugs Administration in 1994, defining 4.0 ng/ml as the cut-off,[36] which remains unchanged. However, PSA screening has been the target of many controversies,[36–38] mostly due to the lack of evidence of a reduction in mortality rates,[36] and the test's poor specificity,[16,29,37] which leads to overdiagnosis and overtreatment of patients with latent disease,[29] forcing them to live with the strict consequences of radical surgical treatment, such as pain, impotence, incontinence, infertility and others.[16,37] This limitation of the specificity for cancer can be attributed to the frequent non-malignant disorders affecting many men, including benign prostatic hyperplasia (BPH) and prostatitis, which may cause elevations in serum PSA levels,[39] misleading the diagnosis.

PSA level has also been used in management as a predictor of recurrence after treatment, using the nadir PSA (nPSA) as the baseline for treatment follow-up. The nPSA is the lowest measured PSA post-treatment, usually achieved four to six weeks after RP, and can be used to forecast the patient's outcome. After RP surgery, PSA level should be less than 0,1 ng/mL[40], and should be maintained unchanged. Biochemical recurrence is then defined with a cut-off of more than 0,2 ng/mL following

primary cancer treatment, indicating incomplete resection or metastatic progression.[41] There are several suggestions as to the cut-off in the rise of PSA above the nPSA to define recurrence following RT treatments. Still, many use levels of 0,5 ng/mL or less as indicator of possible recurrence after irradiation treatments.[42] Patients with advanced stage, i.e. metastatic PCa, initially respond well to HT, but many times end up progressing to CRPC. A lower limit of the nPSA of 1,1 ng/mL showed promising results as a predictor to hormone refractory PCa, following hormone therapy (HT).[43]

1.2.3 Treatment

Treatment for PCa ranges from surveillance to radical local treatment, namely RP, with or without lymph node dissection (LDN), external beam radiotherapy (EBRT), chemotherapy or adjuvant/HT, for example ADT.[18,32] The treatment strategy is defined according to initial PSA serum level, disease grade, the patients age and general condition, and family history.[16,32] For patients with advanced disease, such as metastatic patients, included in the high-risk group, the most commonly used, and recommended, treatment is hormonal therapy combined with RT.[16,32,44] These patients need to be highly surveyed in order to perceive if the cancer progresses to a more aggressive state, named androgen-resistant or CRPC.[32,45]

1.2.3.1 The importance of Radiation Therapy and dose administration

RT plays an essential part in cancer treatment and contributes to the cure or palliation of many cancer patients. Is used to treat up to 50% of cancer patients and is responsible for 40% of management of cured patients.[46–48] The ultimate objective of curative RT is to eliminate all cancer stem cells (CSC), the ones capable of recurrence, in the primary tumor and adjacent lymph nodes, or in oligometastatic (OM) disease, while limiting the impairment caused in normal healthy tissues.[48,49] Over the past decades, developments in RT technology, such as intensity-modulated radiotherapy (IMRT), image-guided radiation therapy (IGRT) and stereotactic body radiotherapy (SBRT), have allowed improved precision in the delivery of radiation and dose escalation, while decreasing the associated morbidity.[50] Conventional fractionated RT, which consists in dividing the prescribed radiation dose over several treatment sessions, resulting in a dose escalation[32,50,51], is the suggested approach using radiation treatments.[32,33] This RT treatment usually involves the delivery of single 1.8 to 2 gamma rays (Gy) fractions, 5 days per week for 8/9 weeks, resulting in a total dose of 76 to 80 Gy.[32,50,51]

1.2.3.1.1 Hypofractionated RT and its advantages

For clinically localized PCa there are some studies supporting RT treatment using hypofractionated SBRT,[50,52] consisting in the delivery of doses in smaller fractions, in response to the more sensible nature of this tumors.[50,53] The application of this hypofractionation technique is now possible due to the technological advances in image-guided treatment delivery systems, making it possible to precisely apply radiation into the tumor, while massively minimizing the radiation dose to the surrounding tissues, resulting in a better tumor control.[47,50,52] The introduction of advanced imaging systems, such as positron emission tomography (PET), computed tomography (CT), magnetic resonance imaging for gross tumor volume (GTV) delineation and the ability to verify the accuracy of the treatment in real time with IGRT, have contributed greatly to the amazing evolution and success of RT treatments.[53] For OM-PCa patients, trials have shown that the application of radiation in a single fraction, single dose radiotherapy (SDRT or SD-IGRT), namely one dose of 24 Gy instead of 3 fractions of 9 Gy,[51,53] has advantages in controlling OM tumors, resulting in better overall outcomes.[52–54]

1.3 PCa metastasis

The ability that cancer cells have to disseminate and form metastasis, in a complex multistep process, colonizing distant tissues and organs, is what makes cancer an unpredictable and deadly disease, responsible for 80-90% of cancer-related deaths.[55–58]

1.3.1 The oligometastatic state

The state of tumor development is reflected in the likelihood, number and sites of the metastasis,[59] and PCa patients are divided into two groups according to the number of metastasis, namely polymetastatic (PM) or oligometastatic (OM).[54] Hellman and Weichselbaum first proposed a clinically significant state of oligometastasis in 1995,[59] defining it as an intermediate state of cancer spread between localized and widespread metastatic disease, where a patient has a limited number of distant metastasis, up to five lesions, and where the primary tumor can be in a controlled state.[54,60–62] The treatment strategy for OM-PCa is not clear due to the lack of uniformity in describing the condition,[60] however, the idea of OM disease has its foundation around a stepwise progression where a cancer initially metastasizes in a limited way, before acquiring the capability of a widespread PM disease, with more than five metastasis.[60,63] Contrary to widespread PM disease, OM patients may benefit from metastasis-directed local treatment. [61]

1.4 Biomarkers, PCa diagnosis and management

1.4.1 The need for new biomarkers: state of the art

Regarding the biomarkers used for PCa diagnosis, prediction and management, it's clear that the currently used diagnostic tests provide limited information regarding the progression potential of a patient's cancer.[64] Thus, there is an urgent need for novel biomarkers that can be used to stratify PCa aggressiveness, differentiating between low and high-risk disease, complementing serum PSA test, and providing a more precise tool in clinical management.[4,29,36,38] There are already many promising biomarkers for PCa, known for being implicated in the progression of the disease. Biomarkers such as the α-methylacyl coenzyme A racemase (AMACR), the AR gene, prostate-specific membrane antigen (PSMA), RNA markers,[65–68] and more recently, epigenetic alterations[29] have been targets of interest. AMACR is an enzyme that plays a critical role in the peroxisomal beta oxidation of branched chain fatty acid molecules, can be found in molecular vesicles in the cytoplasm,[69,70] and has been associated with higher PCa risk and aggressive disease.[36,71,72] After its discovery, this biomarker started being used in clinical pathology as a combined immunohistochemistry (IHC) test with p63, allowing a clearer differentiation between normal glands and cancer, the later characterized by expression of AMACR and loss of p63 due to lack of basal cells.[36,70] The AR gene has long been suggested as the possible mediator for androgen-independent progression,[73,74] leading to CRPC, due to the different variants, mutations and polymorphisms that have been and continue to be found in PCa.[73,75–78] This gene comprises three domains: a N-terminal domain, a central DNA-binding domain and a C-terminal ligand-binding domain (LBD),[79] the latter controlling the activation and transportation of the AR protein from the cytoplasm to the nucleus, upon ligand binding followed by a conformation change. When unligated to androgens, the AR remains retained in the cytoplasm, in an inactive form. However, some PCa tumors express the alternative spliced variants, namely the AR-V7 (AR splice variant 7), the most commonly found variant, in which the truncation leads to a lack of the LBD domain. Therefore, the cells no longer require ligand binding for nuclear localization and can mediate AR activity that confers resistance to ADT, such as Abiraterone and Enzalutamide drugs, thus leading to the aggressive CRPC phenotype. PSMA is a type II transmembrane glycoprotein that can be found mostly on prostate epithelial cells and it's not secreted, contrary to PSA.[80–82] This protein has gained increased attention as a prognostic PCa marker because it

is commonly found up-regulated in cancer cells, correlating with high tumor grade and high risk of advanced disease.[83–87] PET-CT using PSMA as target for imaging has gained interest in management of PCa patients,[88,89] due to the lack of specificity of probes targeting PSA.

1.5 Anatomic pathology and personalized medicine

Nowadays, the practice of diagnostic anatomic pathology often generates fragmented information, but pathology diagnosis in the context of personalized medicine has progressed to a more evidence-based practice, resulting in the creation of many tests performed in tissues or molecularly, providing information about the prognosis and response to therapy. However, the information that can be extracted from histological slides (Figure 1.1A), paraffin blocks and formalin-fixed paraffin-embedded (FFPE) sections, has much more to give that what is being currently used in clinical pathology.[90–92]

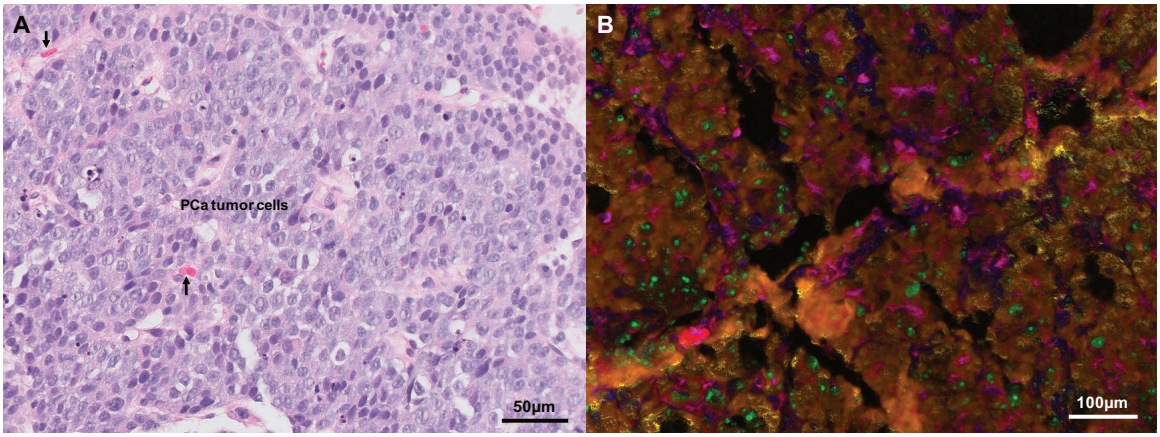

Figure 1.1. Representative images for histological slides with H&E (A) and IF (B) staining methods. Image A displays a classic H&E slide image of a prostate tumor, which is the currently imaging method used for pathologists in PCa diagnosis. Image B corresponds to the multiplex IF staining of the same patient case as image A. Arrows in image A: red blood cells.

1.5.1 Systems Pathology: an uprising prediction tool for PCa management

Based on this, the concept of Clinical Systems Pathology was created several years ago.[92] This methodology consists in compressing data of image analysis, pattern recognition, and biomarker multiplexing imaging,[93,94] by creating an integrated and multidisciplinary methodology as a possible predictive clinical diagnosis tool, incorporating information that goes beyond pattern recognition, such as Gleason grade. It could, eventually, have an application in personalized medicine by incorporating tumor diagnosis, patient prognosis and possible prediction of response to treatments, as well as the probability of experiencing a specific outcome over time.[91,95,96] Many of the studies applying the Systems Pathology model used PCa as the cancer prototype,[93–97] since this type of cancer is lacking good prognosis prediction tools. This model provided a way to use FFPE sections in a reliable way, extracting quantitative phenotypic data from them, by the development of a quantitative multiplex immunofluorescent (IF) spectral approach that measures biomarker expression levels in FFPE cuts using fluorescent tagged antibodies (Figure 1.1B).[94–96] Thus, this resulted in some tissue-based, molecular-driven assays that provide information regarding prognosis and response to therapy of PCa patients, representing a major advance in the standard practice of tissue-based pathology.[90–92,95]

1.6 Circulating cell free DNA as a liquid biopsy for cancer

During tumor formation, cancer cells are discharged into the circulation, known as circulating tumor cells (CTCs). The breaking of tumor cells, both in the primary tumor and CTCs, and from cells

of the tumor microenvironment, leads to the release of circulating cell-free DNA (cfDNA) into the bloodstream.[98,99] The cfDNA consists of highly fragmented DNA strands, with lengths between 180 and 200bp,[99] and is found with increased concentrations in cancer, and is associated with tumor progression.[100,101] Another step towards precision medicine is the liquid biopsy, consisting in the quantification and molecular analyses of cfDNA from blood samples.[102] This concept has gained significant attention in the cancer field especially as a tool for biomarker discovery, aiming to use this as a diagnostic, replacing invasive techniques such as tissue biopsies, and follow-up tool,[99,101–103] for it delivers the possibility of taking successive blood samples at several time-points, consequently allowing the tracking of changes in cfDNA during the natural course of the disease and/or during cancer treatment.[99,101,102]

1.7 Quantitative analysis of biological images

Over the last years there has been a great increase in the amount of bioimaging informatics tools available, differing in their intended application, usability, openness and costs. Imaging software for biological analysis allow the extraction of biologically meaningful quantitative data from microscopy images.[104,105] There are multiple open-source software options for image analysis namely ImageJ™, CellProfiler™, inForm® Cell Analysis™ (PerkinElmer) and QuPath™[106]. From these, inForm is the only application that is not open, its algorithms enable a quantitative per cell analysis of IHC and IF images in single and simple multiplex assays. This software also allows tissue and cell/object segmentation, based on the tissue morphology, for example stroma versus epithelium, and on the cellularity, segmenting cells in nucleus, cytoplasm and membrane. Phenotyping of cells is also possible using the images' spectral data. CellProfiler and QuPath are both versatile and easy-to-use open-source platforms, that allow exploring, analysing data from image-based experiments and performing cell-based quantitative analysis, such as cell counting and classification. Above all, QuPath is a platform developed for pathology image analysis, and as so, allows a quick pathological analysis and biomarker interpretation for whole slide H&E or IF image analysis.

2 HYPOTHESIS AND PROJECT GOAL

Our hypothesis contemplates that a OM-PCa state exists that corresponds to an early metastatic stage and presents specific molecular alterations. This project consists in a pilot study in which, using retrospective clinical data, and genomic and phenotypic signatures, we are aiming to generate a novel diagnostic algorithm to define the molecular characteristics of OM-PCa. This will allow the selection of candidates with OM-PCa for a treatment approach that renders long-term disease-free and higher overall survival in settings presently associated with dismal prognosis. The main goal of this project is to analyse some OM-PCa cases searching for differences in the molecular phenotype of metastatic versus primary prostate cancer (on biopsy or prostatectomy samples) from alive and deceased patients, by using a quantitative multiplex IF approach.

3 PATIENTS AND METHODS

3.1 Subjects and samples

This study was approved by the Ethics Committee of the Fundação Champalimaud: all patients whose specimens were used for the experiments performed in this thesis had signed a consent permitting the use of their biological samples for research purposes, for this project and future related projects. The study cohort consisted of men with OM-PCa, with up to three metastatic lesions, and most of them presented with two or three metastases. However, as it's very common in cancer treatment management, some of the patients were not biopsied for their metastasis since this would include an extra procedure which sometimes is not needed since there was no doubt regarding the nature of the lesion (for example, an increase in PSA in a patient with a previous PCa, whose PET-CT shows appearance of new lymph nodes, which are labelled with PSMA). In these cases, the patients are treated right away either with hormonal, chemo or radiotherapy. As so, we managed to analyse eleven samples from eight patients (Table 4.3) out of the 29 OM-PCa cases initially identified, six of them from metastatic sites. The eleven FFPE blocks were sectioned in the Department of Pathology of the Champalimaud Clinical Centre, resulting in sections of 5 μm, that were used for the multiplex IF assay.

3.2 Multispectral Microscopy

Fluorescence images were acquired using a CRI Nuance multispectral camera mounted on a Nikon 90i automated fluorescence microscope (at magnification 200x), and controlled by MetaMorph software. DAPI was recorded between 460 and 480 nm, Alexa 488 was captured between 510 and 560 nm in 10 nm intervals. For the Alexa 647, recorded between 640 and 710 nm, and Alexa 555, recorded between 560 and 630 nm, custom-made long pass filters were used, as previously specified.[94,96] Both Alexa 594 and 568 were captured using the same filter, recorded between 580 and 650 nm (Figure 4.2). Specific regions of interest (ROIs) were selected using the Nuance software for image analysis, to create a spectral library necessary for the spectral un-mixing process of the images. The background noises were detected and removed, obtaining an image with all biomarkers' individual fluorophore signals. Two multispectral libraries were created, one for a faint DAPI and other for a strong signal, to prevent losing the DAPI information in tumor areas where other nuclear biomarkers could mask the signal.

3.2.1 Quantitative Multiplex biomarker immunofluorescence assay

We used a previously reported multiplex IF spectral assay optimized as a penta-plex image generated at Mount Sinai, NY,[94,96] that analysed the presence of the chosen PCa characteristic biomarkers in FFPE sections using fluorescent tagged antibodies, allowing the visualization of multiple antibodies in a single tissue section. For this project, we modified the previously reported multiplex interchanging one of the markers (described in the results section). Our new IF protocol integrated five antibodies (Table 3.1), organized and incubated in three antibodies sets (Table 3.2).

Table 3.1. List of all primary antibodies used for the multiplex IF protocol.

Antibody name	*Clone*	*Source*	*Catalog #*	*Company*
AMACR (13H4)	Monoclonal	Rabbit	M3616	Dako
Androgen Receptor (D6F11)	Monoclonal	Rabbit	5153S	Cell Signalling
PSMA (1D6)	Monoclonal	Mouse	NCL-L-PSMA	Leica, Novocastra
Cytokeratin 18 (E43-1)	Monoclonal	Rabbit	Ab32118	Abcam
Ki-67 (MIB-1)	Monoclonal	Mouse	M72401	Dako

All primary antibody sets are incubated for 1 hour at room temperature, followed by incubation of the secondary sets for 30 min, also at room temperature. The first antibody set consists of AMACR (1:1500) and PSMA (1:50), the second antibody set is with CK18 (1:100) and Ki-67 (1:300), and the third and last antibody set consists only of AR (1:100). All secondary antibodies were diluted to 1:100, except R647 that was 1:50.

Table 3.2. Antibody sets used for the IF multiplex assay in a multistep protocol. In each antibody set the primary antibody/ies was/were incubated first, followed by the secondary, and then another antibody set, using the same method (R stands for rabbit, M stands for mouse)

Antibody set	*Primary antibody*	*Secondary antibody*
1	AMACR	Alexa Fluor R594
	PSMA	Alexa Fluor M555
2	CK18	Alexa Fluor R647
	Ki-67	Alexa Fluor M488
3	AR	Alexa Fluor R568

For the multi-step staining, the FFPE sections were first dewaxed, followed by an antigen retrieval step, that were performed in an automated Bond staining machine (Bond MAX, Leica Biosysytems), and then followed by the manual IF (Figure 3.1). FFPE sections of a PCa lung metastasis were subjected to the same quantitative multiplexing IF assay as a positive control for the staining.

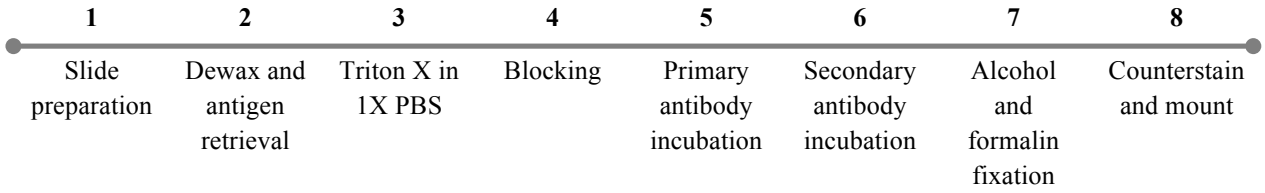

Figure 3.1. Scheme of the multistep protocol for multiplex IF. Steps 1 and 2 are performed in the Pathology Department. Steps 5-6 are repeated for each antibody set, meaning that the antibody set 1 is applied, primary and secondary, followed by antibody set 2 and 3, in the same way. Washes with Bond Wash (Leica Biosystems) were performed between the antibody incubations.

3.2.2 Multispectral library

The multispectral library (Figure 4.4) was constructed using specific tissue staining and the Nuance software for correct spectra isolation.

3.2.3 Image Analysis

Multiple images of tumor regions were acquired for each patient, followed by an analysis of small selected regions of interest (ROIs) or using the whole image when tissue was small. For each sample, a minimum of five images were analysed, with a mean of 832 cells analysed per sample. Depending on the density of cells in each metastasis, more images were analysed, if necessary. The evaluation of the levels of expression of the markers was performed using an open software, QuPath, by doing a semi-automated counting of cells and obtaining the values of percentage of cells expressing each biomarker (supplementary data: Figure 8.2 and Figure 8.3). For the cytoplasmic markers, a cell was counted as expressing the marker if there was signal present in the cytoplasmic regions surrounding cell's nucleus. A trial for the QuPath system was performed, comparing results and ensuring the reproducibility of the analysis. All images were scaled using ImageJ.

The analysis of the images was adapted to the different tissues where the tumor was located, either lymph node, lung, bone or suprarenal gland, because the markers are differently expressed in the different tissues and some unspecific expression can sometimes be found. Above all, the tumor appeared distinctively in the different metastasis so, to correctly identify the tumor, it's necessary to use

empirically recognition of the characteristics of prostate tumor cells. These characteristics include the size of nuclei, higher ratio nuclei/cytoplasm, and multiple and visible nucleoli.

3.3 DNA and RNA extraction from FFPE sections

DNA and RNA were extracted using the MagMAX™ FFPE DNA/RNA Ultra Kit (ThermoFisher, #A31881), according to the manufacturer's instructions. This kit uses magnetic beads to extract DNA and then RNA. It starts with a step of deparaffinization of the FFPE slides with xylene and alcohol, followed by the extraction of the nucleic acids.

3.3.1 Quality assessment of DNA by PCR

A quantity of 10 ng of DNA was used to run a PCR of CENP-A (primers are summarized in Table 3.3), to assess the quality of the extracted DNA. Amplification consisted of an initial denaturation for 3 minutes at 94ºC, followed by 35 cycles of melting at 94ºC for 30 seconds, annealing at 60ºC for 30 seconds and extension at 72ºC for 35 seconds. After PCR, DNA was quantified using the Nanodrop™ 2000 platform for quantity and quality. The PCR product was run in a 2% agarose gel containing GelRed dye for presence of a band of 548bp.

Table 3.3. Forward (Fwd) and reverse (Rev) primer sequences for the housekeeping genes CENP-A and GAPDH.

Primers	*CENP-A*	*GAPDH*
Fwd	GGAACTCTCTCGTTTGTCCACCTTAG	CAGCCTCAAGATCATCAGCA
Rev	GGGCTCAAAGGATTGTAGGAAAG	GTCTTCTGGGTGGCAGTGAT

3.3.2 Quantitative real-time PCR and conditions

A quantity of RNA of 1µg for each sample was converted into cDNA using SuperScript III First-Strand Synthesis kit (Invitrogen #18080-051) according to the manufacturer's instructions. RNA concentration was quantified using Power SYBR Green PCR Master Mix (Applied Biosystems Biosystems #4367659) according to the manufacturer's instructions. Reactions were carried out in 96-well PCR plates using the Bio-Rad CFX96 system for qPCR measurement. Amplification consisted in an initial denaturation step for 15 min at 95 ºC, followed by 40 cycles of melting at 94ºC for 30 seconds, annealing at 60ºC for 40 seconds and extension at 72ºC for 40 seconds. All samples were run in triplicates, using the housekeeping gene GAPDH (Table 3.3) and a positive control cDNA.

3.4 Statistical analysis

Excel was used for data organization, and GraphPad Prism 6 was used for graph construction and statistical analysis. The data from single samples is presented as mean and standard deviation, and for the comparison between different samples from the same patient we used a multiple student's t-test for paired samples, followed by a Sidak-Bonferroni multiple comparison method (****, ***, ** and *, denotes p-value <0.0001, <0.001, 0.001-0.01, and 0.01-0.05, respectively). A nonparametric Spearman rank correlation test was used to evaluate the correlation between different qualitative, clinical and pathological, variables, and the quantitative values for the biomarkers expression levels (two-tailed test, CI 95%). Kaplan-Meier curves representing the percentage of patient survival were performed by stratifying the patient's samples using the median expression for some biomarkers and clinical data (Log-rank Mantel-Cox test for significance, p-value<0.05).

4 RESULTS

4.1 OM-PCa cases studied

From a cohort of 29 OM-PCa patients treated in the Department of Radiation Oncology at the Fundação Champalimaud, we managed to get eleven FFPE tissue samples from a total of eight patients which corresponded to one prostatectomy, four prostate biopsies, and six metastasis.

4.1.1 Characteristics of first metastatic site and grading of the primary tumors

The most common first metastatic site was the lymph nodes (LN) (Figure 4.1A), which occurred in four patients (57,1%). The other corresponded to one metastasis in the suprarenal gland (SR), very unusual (14,3%), and two to the bone (BM) (28,6%). Out of the metastatic samples, two belonged to the same patient, number 18 (Table 4.3). From seven out of the eight patients studied, we got the information regarding the GS of the biopsy samples. We observed that the most commonly attributed GS was of 6 (3+3), with a frequency of 28,57% (n=2) (Figure 4.1B).

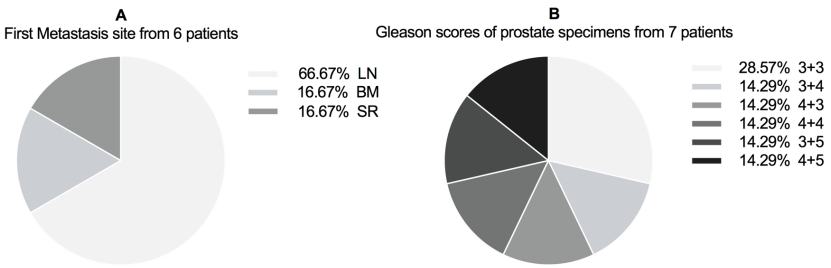

Figure 4.1. Pie charts summarizing the most common site for first metastasis (A) and the GS of the prostatectomy or prostate biopsy specimens from seven patients (B).

Table 4.1. Clinical and pathological characteristics of the eight OM-PCa patients at the time of diagnosis. iPSA stands for initial PSA and cTNM is the clinical TNM staging of the tumor.

Variable	*Total (n)*
Number of patients	8
Age, years:	
Mean	61,9
Range	57,1-66,7
iPSA, ng/mL:	
Mean	11,3
<10	3
10−20	2
≥20	2
Missing	1
Gleason Score:	
≤6	2
7	2
8	2
≥9	1
Missing	1
cTNM:	
T2	4
T3	1
T4	1
Missing	2
Clinical follow-up, months:	
Mean	90,7
Range	20,9-163,9

4.1.2 Clinical and pathological characteristics of the primary lesions

The clinico-pathological characteristics at diagnosis for all patients are summarized in Table 4.1. The mean age and PSA at diagnosis was of 61,9 years, and 11,3 ng/mL, respectively. Most of the patients (50%) presented a clinical TNM tumor staging of T2, meaning that the tumor is palpable by DRE and still confined to the prostate. One patient was diagnosed with a very advanced tumor stage, T4N1, where the tumor had grown into tissues adjacent to the prostate, and spread to one or more LNs.

After the initial diagnosis, the great majority of the patients underwent hormone therapy (HT) or RP (Table 4.2). The most commonly used drugs for HT in PCa treatment are Zoladex, Bicalutamida, Abiraterone and Denosumab, all of them suppressing the production of sex hormones. As for the second and third treatments, the most common is RT, either SBRT or SDRT. Also in Table 4.2, we can see that six of the patients were treated with SDRT, and especially patient 29, whom was treated exclusively with SDRT for all metastasis. Out of the eight patients, three died of the disease, patients 10, 22 and 27, resulting in a mean age at death of 69,5 years. These patients were managed and remained alive during a period of 8, 6 and 14 years, respectively. The mean time from the diagnosis to the first RT treatment was of 63 months (range 9,7 – 147,6 months) and from diagnosis to death or last visit (clinical follow-up) was of 91 months (range 20,9 – 163,9 months; Table 4.1), approximately 8 years.

Table 4.2. Clinical treatment, tumor progression and follow-up management of the eight patients. CT – cryotherapy; RP – radical prostatectomy; EBRT – external beam RT; SDRT – single dose RT; SBRT – stereotactic body RT; WBRT – whole brain RT; BM – bone metastasis; LDN – Lymphadenectomy; LNs – Lymph nodes metastasis; N/A – not applicable; NED – no evidence of disease; DOD – dead of disease; AWD – alive with disease; m – months.

Patient ID	*First Treatment*	*Second Treatment*	*Progression and Third Treatment*	*Status*	*Time from dx to 1st RT (m)*	*Time from dx to death/last follow-up (m)*	*Age at death/last follow-up*
10	Hormone	SDRT (Prostate and Iliac Bone)	SBRT (multiple BM) + Brain progression	DOD	58,2	94,5	70,2
15	Hormone	SDRT (Prostate, Seminal Vesicle and Adrenal gland)	Adrenal and Lymphatic progression	AWD	55,0	90,8	64,7
18	RP	Hormone	SDRT (LNs) + Bone progression + Hormone + Radium 223 + Chemo	AWD	102,2	138,6	78,3
20	CT + Hormone	CT + Hormone	SBRT + LN and BM progression + Hormone + SDRT	AWD	80,8	101,3	74,1
22	Hormone + EBRT	SBRT (LNs)	SDRT (LNs) + Hormone + Chemo + Brain progression	DOD	42,7	76,3	68,3
23	Electroporation + Hormone	SBRT (Prostate + LNs)	N/A	NED	10,9	39,7	60,4
27	RP + adjuvant RT	SBRT (LNs + BM) + CT	Bone progression + WBRT	DOD	147,6	163,9	74,0
29	RP + LDN	SDRT (LNs)	SDRT (LNs)	NED	9,7	20,9	65,8

4.2 IF microscopy and image generation

The IF microscopy technique takes advantage of light emission with different spectral peaks against a dark background. By using indirect IF, the fluorophores are conjugated to a secondary antibody, which is specific for the primary. Biological molecules always emit light at a longer wavelength than that of the exciting light, a phenomenon called Stoke's Shift.[107] The microscope used

has five long-pass filters, and for each, the spectra observed are captured, so that across all filters, the complete spectral properties of each independent signal can be effectively utilized for spectral unmixing (Figure 4.2).

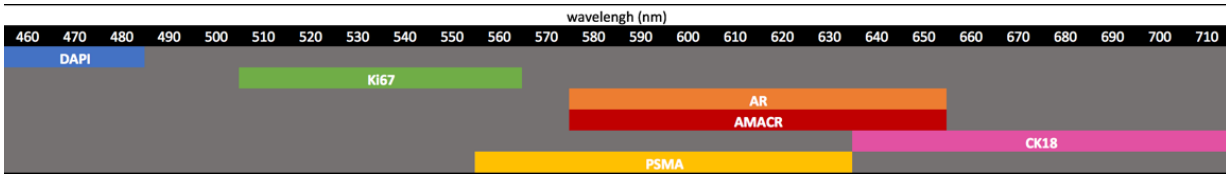

Figure 4.2. Representation of the emission spectra of all the antibodies used in the multiplex IF. The Nuance multispectral camera has five emission filters that allow the excitation of different fluorophores and the image capture of the following emission signal produced by the secondary fluorescent labelled antibody.

The Nuance software was used for raw image visualization, library construction (Figure 4.4) and multispectral unmixing of the scanned images. In Figure 4.3, we can see how from an initial composite image before unmixing (Figure 4.3A), we get a final composite unmixed image (Figure 4.3B), after the software uses the multispectral library to isolate the spectra corresponding to the 5 markers, plus DAPI.

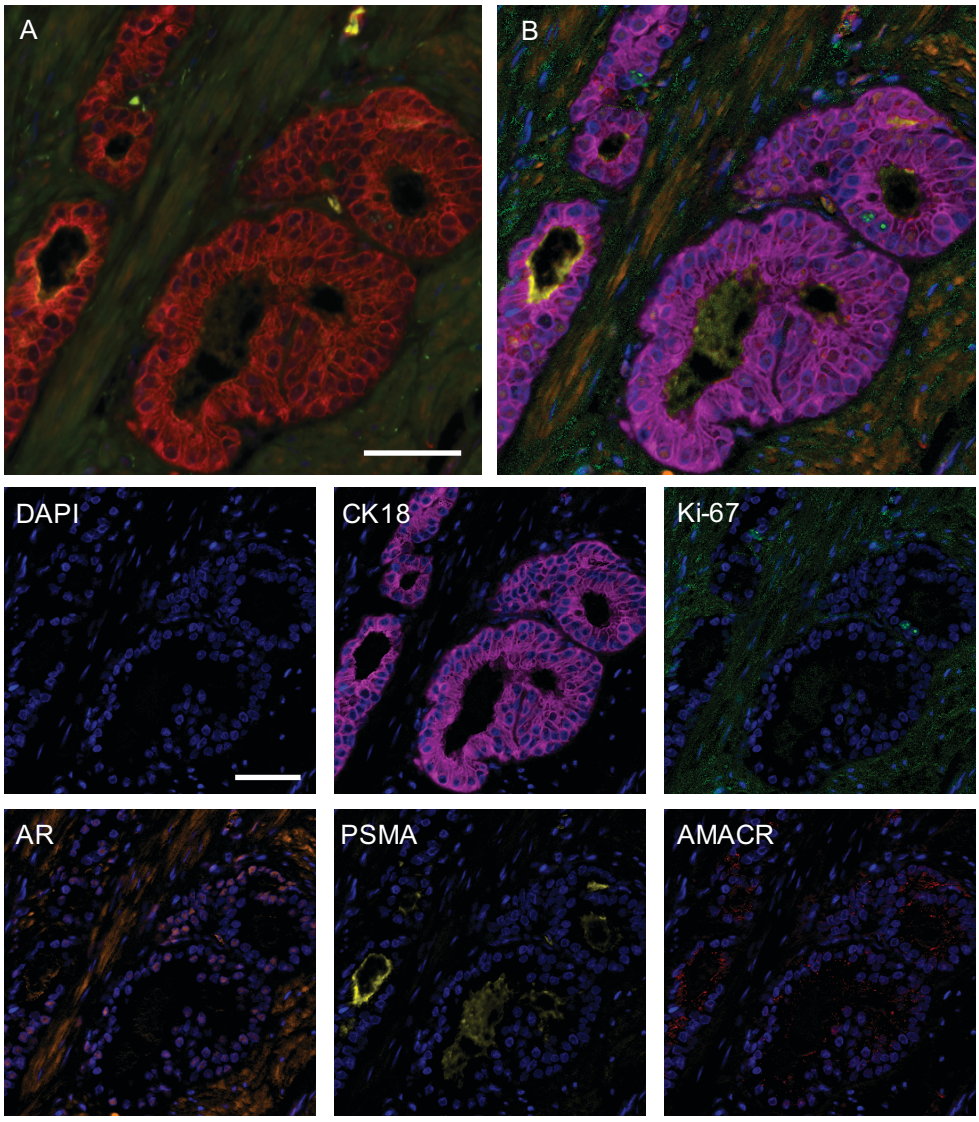

Figure 4.3. Composite IF image of a FFPE section of a PCa prostatectomy before (A) and after (B) unmixing. The six images bellow show the isolated spectra signal for the five biomarkers (CK18, Ki-67, AR, PSMA, AMACR) plus the DAPI. DAPI is in blue, CK18 in magenta, Ki-67 in green, AR in orange, PSMA in yellow and AMACR in red. Scale bars – 100 µm.

4.2.1 Optimization of the multispectral library for the image unmixing process

A multispectral library is what makes sure that the spectrum of interest from each specific marker of interest is separately imaged. Afterwards, the library allows the correct merging of all images together in a final composite. A good spectral library is essential for a reliable unmixing and quantitation of the spectral data. To accomplish this, it's necessary to use a specific stained slides for library construction, so that correct examples of each fluorophore emission spectrum can be acquired, as well as a representative auto-fluorescence. Therefore, we performed double and single staining IF, using the same conditions as the multiplex IF protocol so that we could try to build a clearer spectral library using double-plex (AMACR, PSMA and CK18, Ki-67) and single-plex (AR) stained slides. We managed to construct a good multispectral library that was used to unmix all scanned images, allowing a good image analysis and antibody quantification.

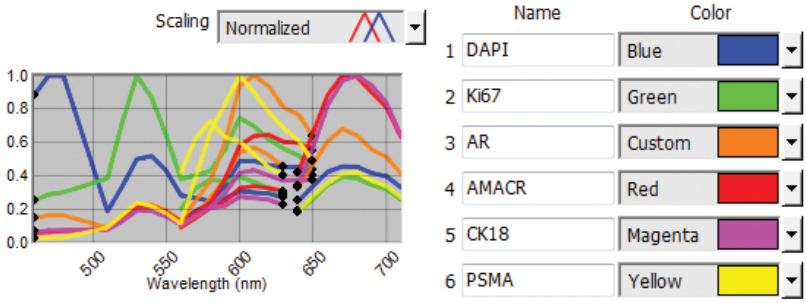

Figure 4.4. Multispectral library spectrum peaks for the five markers plus DAPI (seen on the right), built on Nuance software.

4.3 Background and differences in the signalling between different scanned tissues

While scanning the cases we noticed that the background noise varied greatly according to the tissue that was stained (e. g. prostate, lung, lymph node or bone marrow). Because of this, an experienced pathologist helped with sorting amongst specific signalling and false signal, background noise or auto-fluorescence. Many biological materials are naturally fluorescent, what is called auto-fluorescence, and FFPE derived sections also show increased background due to the paraffin embedding the tissue, but this shouldn't interfere with specific fluorescence labelling. To prevent this, auto-fluorescence is posteriorly removed with the spectral unmixing as unwanted background.

4.3.1 Image analysis and background noises between different metastasis sites

From the eight patients, we got metastasis from three distinct places in the body (Table 4.3): suprarenal, lymph nodes and bone (pelvis and vertebrae).

Table 4.3. Patients ID and list of all the eleven samples that were analysed for each patient. SR – Suprarenal metastasis; LN – Lymph node metastasis; BM – Bone metastasis.

Patient ID	*Primary sample*	*First metastasis*	*Second metastasis*
10	Prostate biopsy		
15		SR	
18		LN	BM
20	Prostate biopsy		
22	Prostate biopsy	LN	
23	Prostate biopsy		
27		BM	
29	Prostatectomy	LN	

We found great and unexpected differences in the final presentation of the unmixed image with all markers, particularly in the lymph nodes stained metastases. In these, the background from the green and yellow filters was always higher, and as so, the image analysis had to be more cautious, correctly

differentiating the antibody correct signal from the background signalling. The bone metastasis were the ones with less background noise, because tumor cells were mostly found in clusters, or mixed with erythrocytes, since these biopsies are of bone marrow.

4.4 Optimization of the IF protocol for the metastasis cases

The original IF multiplex protocol developed at Mount Sinai included Cytokeratin 5/6 (CK5/6) as part of the antibody set one (clone D5/16B4, catalogue #M7237, Dako). CK5/6 is cocktail of high molecular weight cytokeratins expressed by the basal cells of the normal prostatic glands, therefore allowing a quick identification of the normal glands versus PCa, which is characterized by the loss of these cells. Since in metastatic sites, normal prostate tissue is not present, we decided to replace this antibody for another one with interest for the analysis of the metastasis and relevant for PCa management. The choice was between PSA and PSMA, both known proteins in PCa diagnosis and follow-up. The antibody chosen had to be from a mouse source, so that it could be used with the corresponding anti-mouse secondary, the Alexa Fluor 555 (Table 3.2). After some literature review, discussion and evaluation of an IF trial, we settled that PSMA would be more interesting for the analysis of our cases, because it had a heterogeneous distribution along the tumor areas and was expressed only in the lumen of the glands or at the apical region of the cells, not masking the other biomarkers used.

4.5 Case Results

4.5.1 Primary PCa samples: 10B, 20B, 22B, 23B and 29P

In a general way, all primary samples presented a high expression of AMACR and AR, being AMACR more consistent, with values of expression higher than 60% (Figure 4.5 and Table 4.4). Two prostate biopsy samples showed no PSMA expression at all, and through all tumor regions observed (Figure 4.5, 10B and 22B). Ki-67 had zero expression in the prostate biopsies 10B and 20B, and very low expression in samples 23B and 29P, with 0,7% and 0,6% of cells expressing Ki-67, respectively (Table 4.4). PSMA expression was very high in 20B, and of 50% in samples 23B and 29P. In Figure 4.5, graph 22B, we can see that this sample presented the highest Ki-67 value of all the primary tumors.

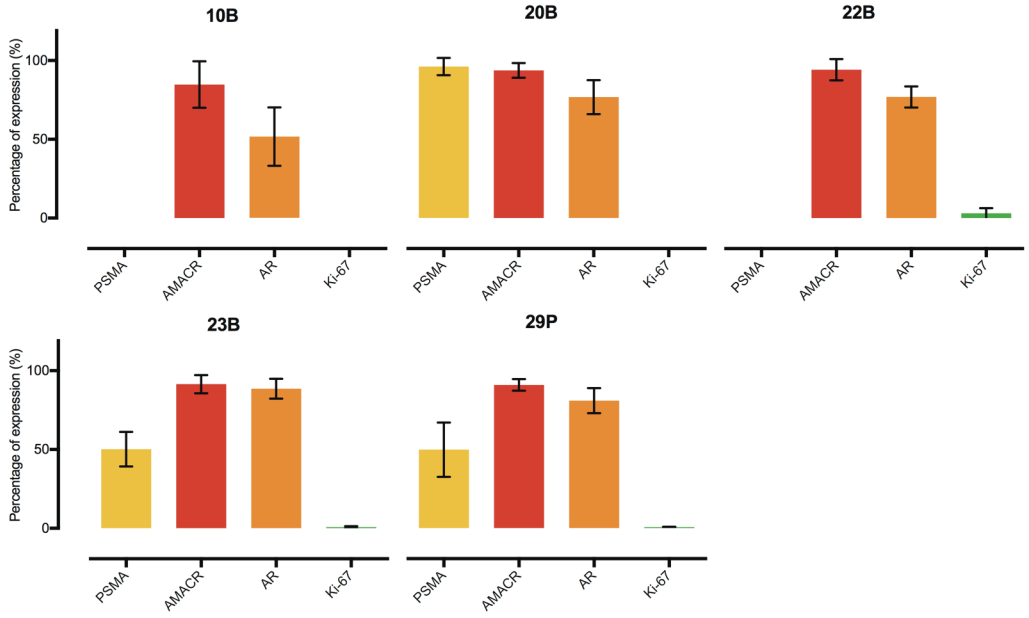

Figure 4.5. Mean percentage of biomarker expression in the primary lesions for all analysed ROIs of each sample/patient. 10B represents patient number 10 and B stands for prostate biopsy specimen. P stands for prostatectomy. 10B, 20B, 22B, and 23B

are all samples from prostate biopsies. 10B – n=5; 20B – n=3; 22B – n=6; 23B – n=5; 29P – n=5, where "n" represents the number of images/ROIs analysed for each sample/patient.

4.5.2 Metastasis samples: 15M, 18M, 22M, 27M, 29M

The analysis of the metastatic biopsies presented different biomarker values compared to the previous primary samples. In Figure 4.6, we can see that from all metastatic samples, the 29M LN metastasis was the one that exhibited higher levels of all antibodies, and in which PSMA, AMACR and AR expression was either 100% or very close (Figure 4.6 29M). PSMA was found highly expressed in 15M, 18M1/2, and 29M, but there was no protein expression in 22M, and 27M displayed low levels of expression as well. The percentage of AR expression was close to 50% in four samples (Figure 4.6 15M, 18M1, 18M2 and 22M, and Table 4.4) of three patients, and overexpressed in the sample 29M. The bone metastasis of patient 27 (Figure 4.6 27M), showed null AR expression, but exhibited the highest Ki-67 value in all metastasis samples, with almost 50% of expression (Table 4.4), which can be visualized in Figure 4.7. Differently, all other samples (15M, 18M1/2, 22M, 29M) had lower Ki-67 percentages, being that the lowest values belonged to 18M1 and 29M.

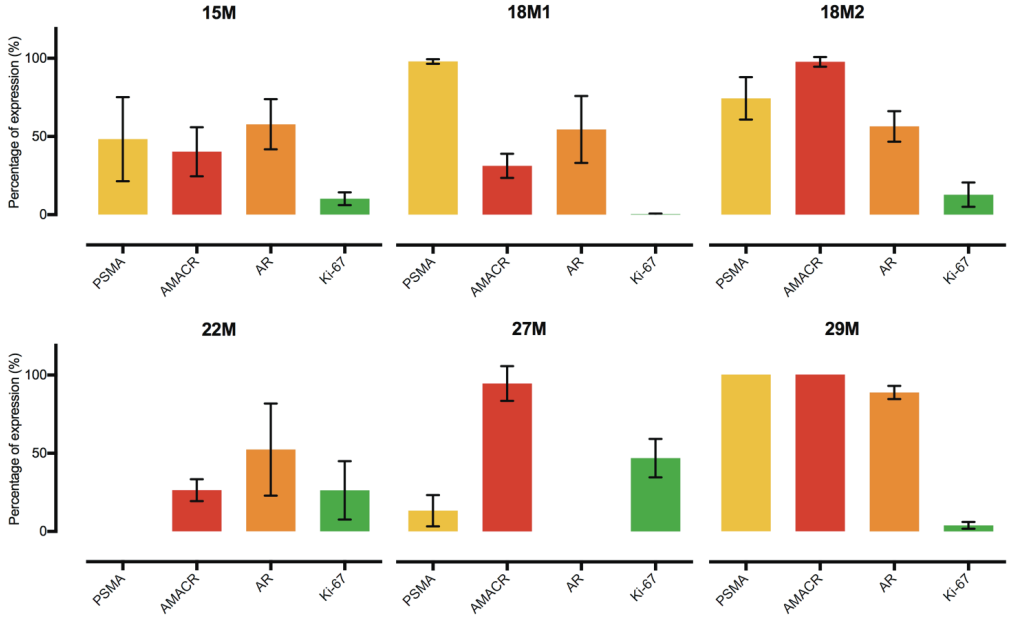

Figure 4.6. Mean percentage of biomarker expression in the metastatic lesions for all analysed ROIs of each sample/patient. 15M represents patient number 15 and M for metastasis specimen. 18M1 and 18M2 stand for first and second metastasis for patient number 18, respectively. 15M – n=7; 18M1 – n=5; 18M2 – n=6; 22M – n=5; 27M – n=9; 29M – n=6, where "n" represents the number of images/ROIs analysed for each sample/patient.

Table 4.4. Mean percentage of cell expression for all analysed samples (n=11), either primary PCa or metastatic lesions.

	Primary lesions Mean % cells expressing				*Metastatic lesions* Mean % cells expressing			
Patient ID	PSMA	AMACR	AR	Ki-67	PSMA	AMACR	AR	Ki-67
10	0,00	84,78	51,59	0,00				
15					48,30	40,24	57,84	10,21
18					97,76	31,22	54,40	0,36
					74,21	97,53	56,33	12,81
20	96,14	93,70	76,74	0,00				
22	0,00	94,30	76,97	3,10	0,00	26,41	52,37	26,29
23	50,19	91,46	88,59	0,71				
27					13,33	94,43	0,00	46,83
29	49,70	90,72	80,75	0,61	100,00	100,00	88,69	3,94

Figure 4.7 shows representative IF images of two very interesting metastases analysed, 15M and 27M. Metastasis in adrenal glands are not commonly seen in PCa, therefore, the 15M sample was a unique case for image analysis. The tissue histology and cellularity allowed to clearly distinguish between adrenal and the much larger, and normally clustered, cancer cells (Figure 4.7A). In this light, the 27M bone metastasis was also a case to take note since it's the only one that exhibited complete loss of AR expression (Figure 4.7B). The AMACR expression is easily recognised as cytoplasmic vesicles and PSMA showed little or non-existent expression.

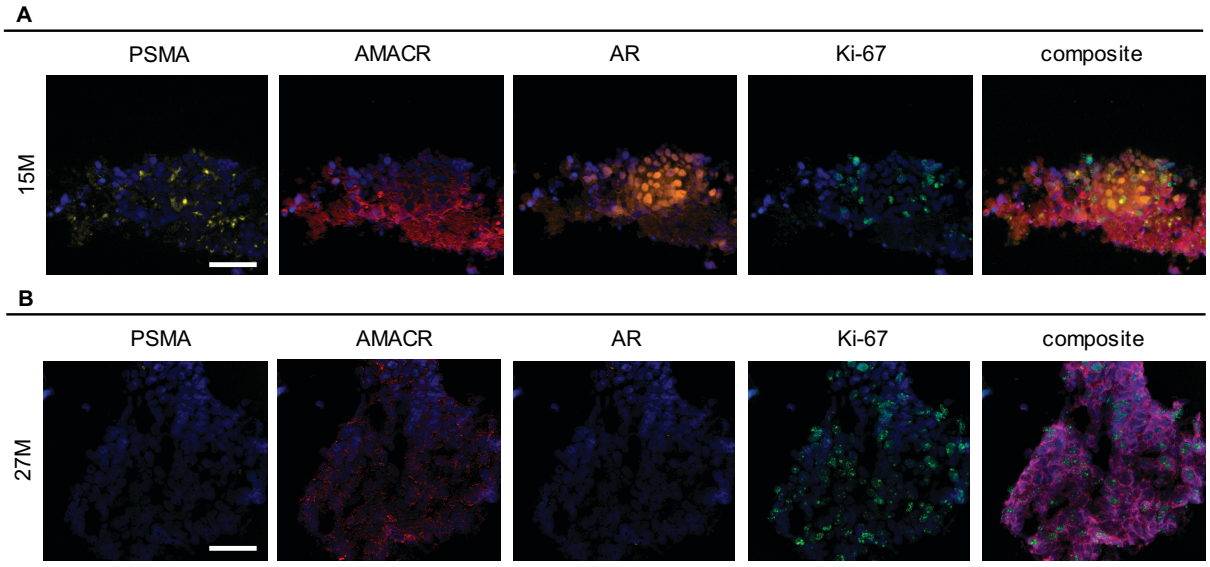

Figure 4.7. Representative IF images for two metastasis cases of two patients. Suprarenal, 15M (A), and bone metastasis, 27M (B) with the isolated spectra images of AR, PSMA, AMACR and Ki-67 (first 4 images), and the final unmixed composite image (last image, right). Scale bars – 100 µm.

4.5.3 Primary PCa and PCa metastasis multiplex IF

Analysis of the mean of all primary lesions, which included the prostate biopsies and the prostatectomy, showed that AMACR was highly expressed in all tissue samples (Figure 4.8A), with little deviation between patients. On the contrary, PSMA showed great variability between the different biopsies. Notably, Ki-67 expression level in the primary tumors was very low, compared with the expression in the compressed data of all the metastasis (Figure 4.8A-C). The metastatic tissues showed even greater variability between patients, presenting results with higher standard deviations, despite the lower sample number. Although we found interesting differences in biomarker expression between the primary and metastatic lesions, the differences were not significant when statistically compared, as displayed in Figure 4.8C.

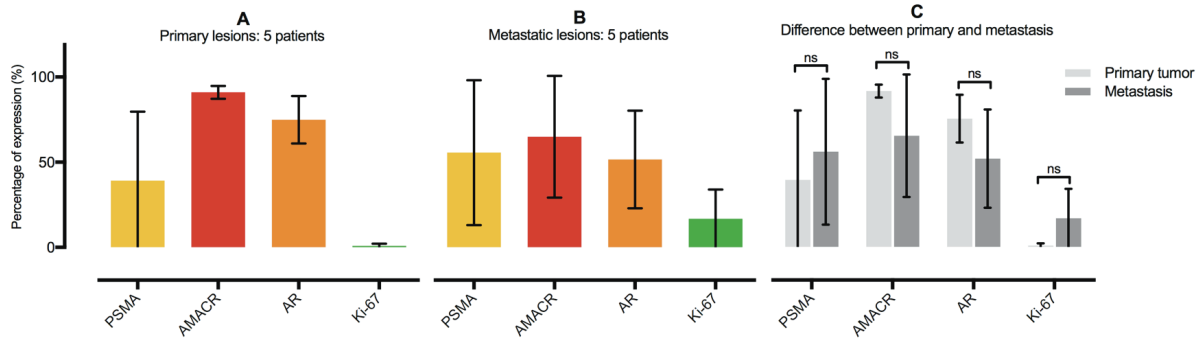

Figure 4.8. Mean biomarker expression of all primary (A) and metastatic (B) samples for the eight patients, (primary samples – patient number 10, 20, 22, 23 and 29, n=5; metastasis samples – patient number 15, 18 (2 samples), 22, 27 and 29, n=6) and

representation of the difference between the biomarkers expression in primary and metastatic lesions (C). Statistical analysis by multiple student's t-test, followed by a Sidak-Bonferroni multiple comparison method. (ns – not significant).

4.6 Comparison between consecutive biopsied patient samples

To perform this comparison, we selected three patients for which we had more than one tissue sample available. Two cases corresponded to primary PCa and metastatic lesion, whereas for patient 18 we had two different metastatic lesions (LN and BM) separated one year, approximately. By comparing these samples, we managed to analyse changes in the tumor phenotype with time.

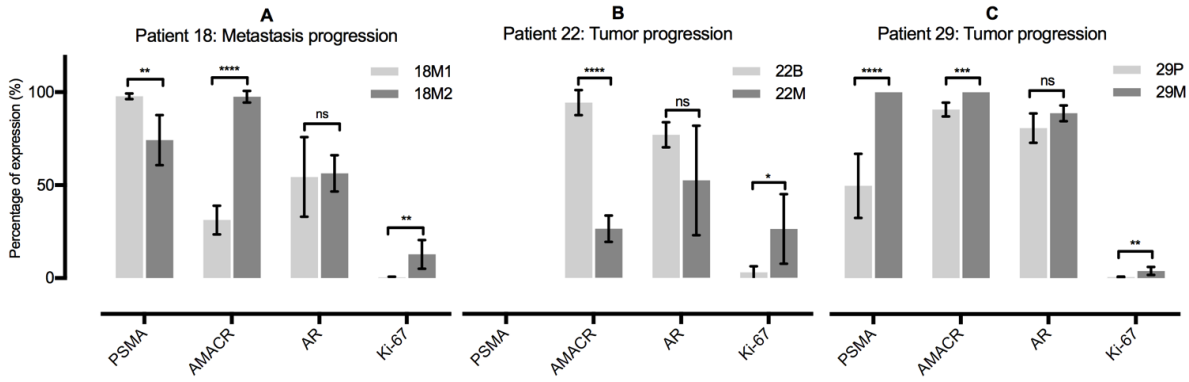

Figure 4.9. Percentage of biomarker expression differences between samples separated by biopsy date. (A) Metastasis progression for patient number 18 and tumor progression, from biopsy/prostatectomy to metastasis samples, for patients 22 (B) and 29 (C). Statistical analysis was performed with the samples biomarkers mean value by multiple student's t-test for paired samples, followed by a Sidak-Bonferroni multiple comparison method (****, ***, ** and *, denotes p-value <0.0001, <0.001, 0.001-0.01, and 0.01-0.05, respectively, and ns stands for non-significant).

Figure 4.9 showcases the differences in biomarker expression between time spaced biopsies for the three patients. For patient 18, we got a metastasis progression, from the first metastasis, 18M1, to the second, 18M2. Patients number 22 (Figure 4.9B) and 29 (Figure 4.9C) allowed the visualization of a more general tumor progression, since the samples analysed were from the biopsy and prostatectomy specimen at diagnosis, and then of the metastasis.

The appearance of the tumor, either structurally or in cell composition, is very distinctive when comparing the scanned IF images from a prostate tissue, LN or bone metastasis (Figure 4.10), and the change in biomarker expression with time is not clear when comparing different tissue metastasis. Comparing the IF images from the first to the second biopsied metastasis for patient 18, it is clear that PSMA expression decreases, whereas Ki-67 increases of expression. In the representative images of 18M2 we see the presence of a higher number of Ki-67 positive cells, some of them showing both AR/Ki-67 expression.

Comparing IF images from a prostate biopsy with a more compact metastatic tissue, such as the LN, allows a simpler visualization of the changes in biomarkers percentage of expression, as we can see with the representative images for the progression of patient number 22 (Figure 4.10B). Neither the 22B nor 22M specimens showed PSMA expression. In fact, the yellow signal seen in the images is background or unspecific signal and it plainly doesn't resemble the normal pattern of PSMA expression, smooth-like expression in the membrane part of the cells, that can be seen in Figure 4.10C (patient 29). AR had a different sub-cellular localization expression pattern in 22M and 29M, as some expression was found in the cytoplasm, rather than just in the nuclei. The LN metastasis of patient 22 was one that presented the highest Ki-67 of our series, and the representative image shows the great amount of proliferation of this metastasis (Figure 4.10B).

The AMACR characteristic granular and cytoplasmic expression is easily seen in patient 29's samples (Figure 4.10C), where this enzyme was overexpressed only in the tumor areas. The tumor cells of the 29M LN metastasis showed a faint AR expression, either in the nuclei, cytoplasm, or in both.

4.6.1 Patient 18: Metastasis progression

Patient 18 showed statistically significant differences in the biomarker expression of PSMA, AMACR and Ki-67 between the first, LN, and second, BM, metastasis (Figure 4.9A). In this progression, all markers increased their expression values except for PSMA. AMACR showed the greatest difference, an increase of about 75% in expression (Table 4.4).

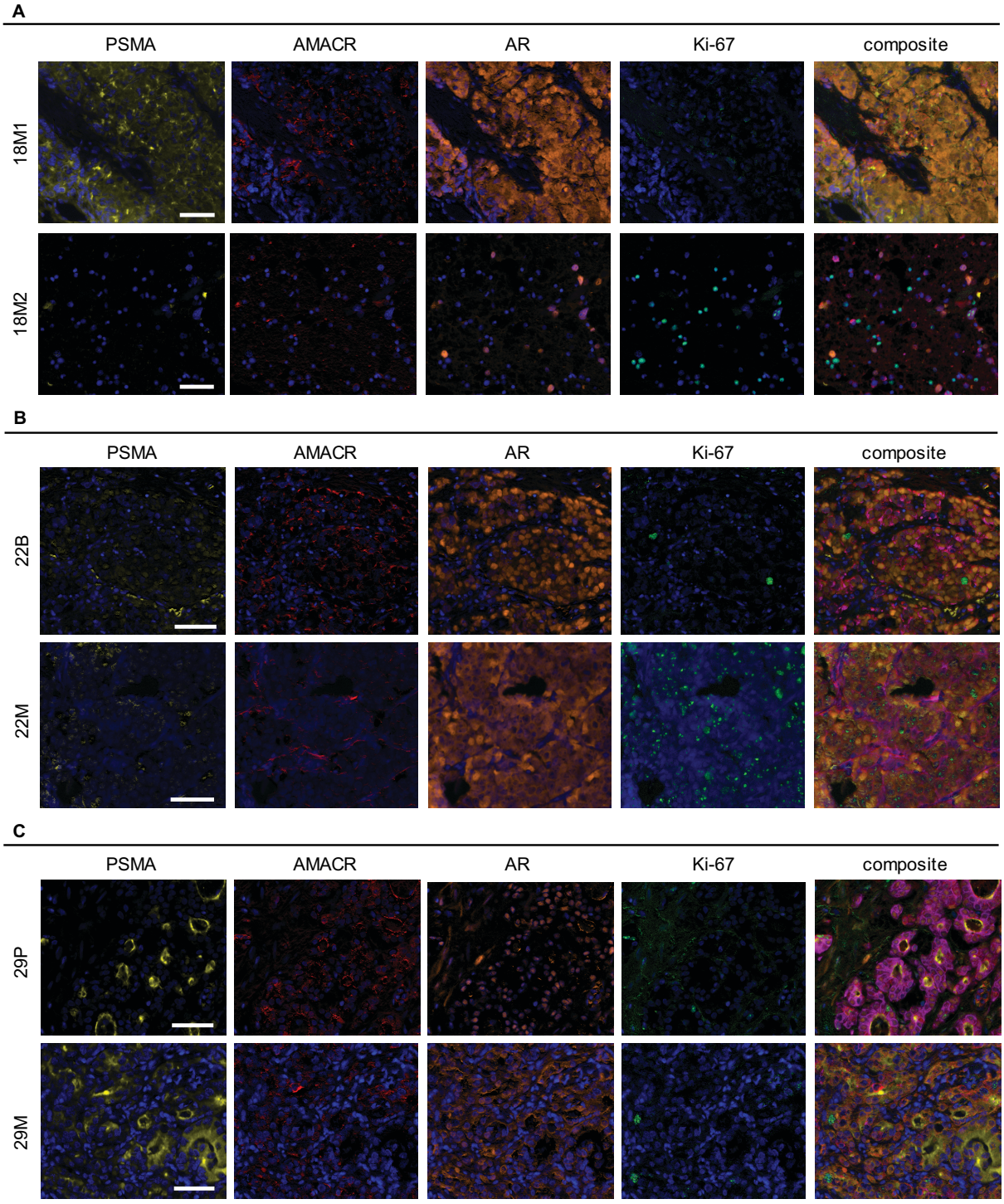

Figure 4.10. Representative IF images of FFPE specimens of primary PCa and metastasis for the three patients analysed. IF Images showing the metastatic tumor progression from 18M1 to 18M2 (A), and tumor progression from 22B to 22M (B), and from 29P to 29M (C). For all of them the isolated signal for the biomarkers of interest is shown first (first four images, from left to right), followed by the composite multiplex image (last image, right). All scale bars – 100 µm.

Figure 4.11 shows that the metastasis biopsies were spaced 1 year, and that the 18M1 was treated with SDRT, displaying a full recovery, but later, at the beginning of 2015, a second metastasis

(18M2) appeared. This metastasis was then treated with HT. Regardless of the treatments, the patient state advanced at the end of 2016, with bone progression, and a great increase in the measured PSA levels (Figure 4.11, graph underneath). In this graph, achievement of nPSA following RP is clearly seen, and then biochemical recurrence is observed when the PSA level elevated.

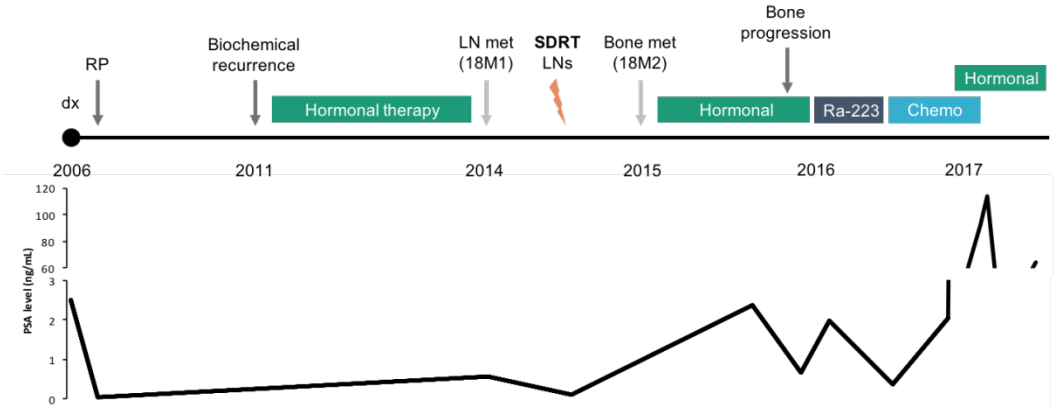

Figure 4.11. Timeline for patient 18 with all important events, biopsies and treatments, the respective dateline and the graphical representation of the PSA level progression alongside the patient's treatment and management. RP – radical prostatectomy, SDRT – single dose RT (24Gy).

4.6.2 Patient 22: Tumor progression

From sample 22B to 22M, PSMA expression remained null and the difference in the AR percentage was not significant (Figure 4.9B). Differently, AMACR showed a great decrease in expression, and Ki-67 proliferative marker also presented a higher value in the metastasis, showing a statistically significant difference.

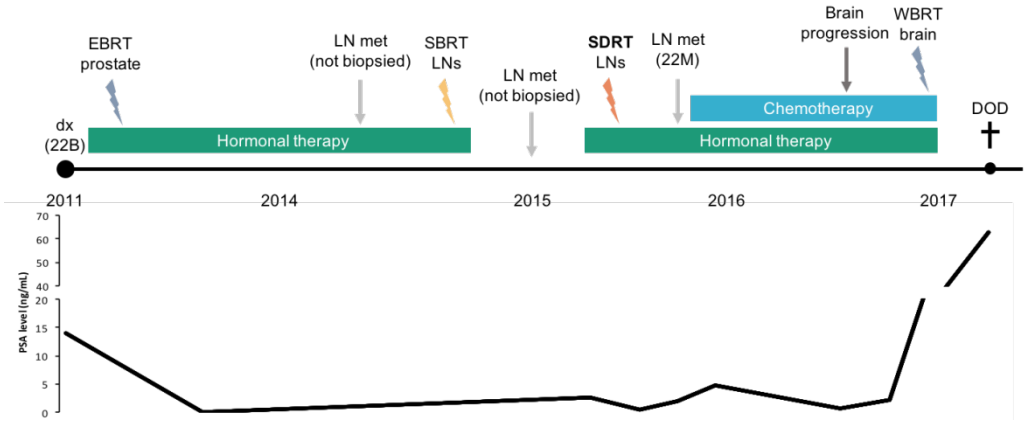

Figure 4.12. Timeline for patient 22 with all important events, biopsies and treatments, the respective dateline and the graphical representation of the PSA level progression alongside the patient's treatment and management. EBRT – external beam RT (24Gy in 5 sessions); SBRT – Stereotactic body RT (24Gy in 5 sessions); WBRT – whole brain RT (35Gy in 5 sessions); DOD – dead of disease.

Regarding the treatments for this patient, Figure 4.12 shows that he undertook HT during a long period of time. As first treatment, this patient received EBRT to the tumor in the prostate along with HT, showing a decrease in PSA (Figure 4.12, PSA graph), reaching the nPSA. The patient remained in a recurrence-free state for three years (2011-2014), until the appearance of the first metastasis. The first two LN metastasis lesions were not biopsied, and were treated with RT, but the following tumor recurrence, another LN metastasis, was biopsied (22M). At the time, the patient was receiving HT, and was put under chemotherapy as a response to the rising PSA and progressing metastization. The advanced state of disease, alongside the appearance of brain metastasis, eventually led to the patient's death.

4.6.3 Patient 29: Tumor progression

Analogously to the other cases, the AR differences between the samples 29P and 29M were not significant (Figure 4.9C), but the other markers showed a great difference in expression. PSMA, for example, increased by almost 50% from the prostatectomy to the LN metastasis, and these samples were collected with a time-lapse of 1 year, approximately (Figure 4.13). The biomarkers AMACR and Ki-67 also showed higher levels of expression in the LN metastasis. Of all patients, patient 29 was the only one that didn't undergo any kind of hormonal or chemotherapy treatment, which are the normal procedures followed for PCa management. Contrarily, after RP and LDN as first treatment, the patient underwent SDRT exclusively as means of dealing with the metastatic progression (Figure 4.13). The PSA levels remained relatively low, not higher than 7 ng/mL (Figure 4.13, PSA graph).

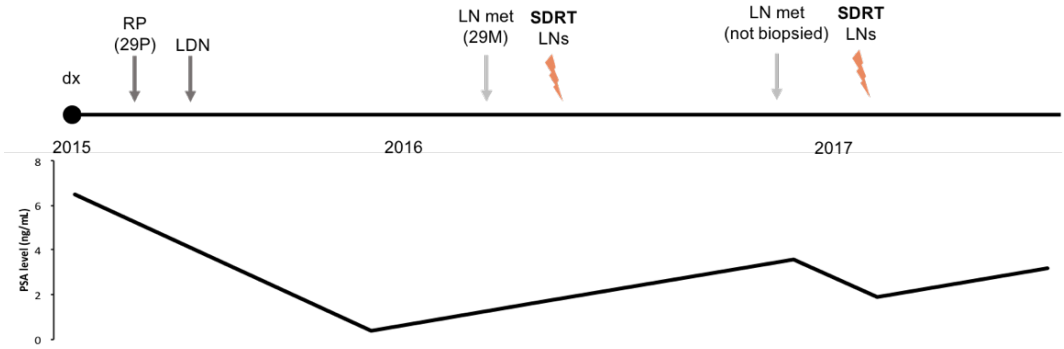

Figure 4.13. Timeline for patient 29 with all important events, biopsies and treatments, the respective dateline and the graphical representation of the PSA level progression alongside the patient's treatment and management. LDN – Lymphadenectomy; SDRT – single dose RT (24Gy).

Interestingly, this patient has been showing complete response to the RT, and remains in a controlled, recurrent-free state of the disease. The nPSA was also reached after primary tumor surgery, although it took more than a few months, and following the last RT treatment a new nPSA is seen.

4.7 Comparison between qualitative and quantitative variables

By comparing the results from the primary samples (n=5), such as the mean biomarker expression, as well as qualitative variables (e.g. iPSA, Gleason score, cTNM, patient status), using the Spearman rank correlation, the results in Table 4.5 display that only AR and iPSA were significantly correlated (also seen in Figure 4.14A). In fact, AR and iPSA were negatively correlated, presenting a rho of -0,9747, meaning that there was a pattern where whenever the iPSA level was low, the percentage of AR expression was high.

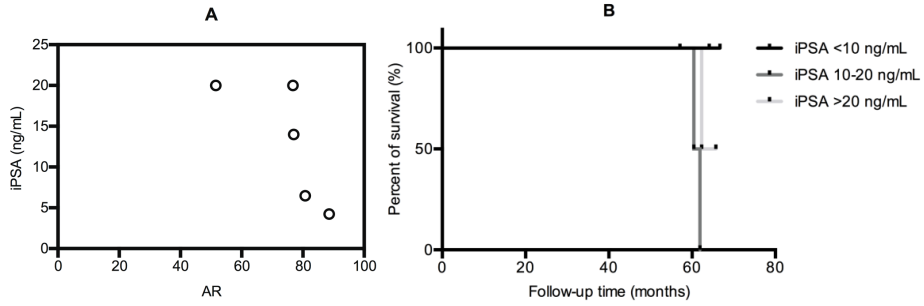

Figure 4.14. Spearman rank correlation (A) of a quantitative, AR, and qualitative, iPSA, variable (r=-0,9747, p-value=0,0333), and Kaplan-Meier curve (B) showing the percent of patient survival for the eight patients stratified by three levels of PSA at diagnosis (Log-rank, Mantel-Cox significance test: Chi-Square: 6,033; p-value=0,0490).

There was no association found between the other markers, and between these and the clinico-pathological data (Table 4.5 and supplementary data: Figure 8.5). The metastasis samples (n=6) also showed no correlation between the mean antibodies expression (supplementary data: Figure 8.7 and Table 8.1).

Table 4.5. Spearman rank correlation using qualitative (iPSA, Gleason Score, clinical TNM and patient status) and quantitative variables (all biomarkers) for all primary lesions (n=5).

	iPSA	*Gleason*	*cTNM*	*Patient status*	*PSMA*	*AMACR*	*AR*	*Ki-67*
iPSA								
r	1	0,1316	-0,2294	-0,4443	-0,1316	-0,0513	-0,9747	-0,6842
p-value		0,85	0,8	0,5	0,8	> 0,9999	*0,0333	0,2167
Gleason								
r		1	0,6309	-0,2962	0,8885	0	0,5774	-0,1481
p-value			0,3	0,7	0,2	> 0,9999	0,4	> 0,9999
cTNM								
r			1	-0,3227	-0,5162	0,4472	0,2236	0,6882
p-value				0,7	0,35	0,5	0,8	0,25
Patient status								
r				1		0	0,5774	-0,1481
p-value							0,4	> 0,9999
PSMA								
r					1	0,2052	0,3078	-0,2895
p-value						0,7333	0,6	0,6
AMACR								
r						1	0,2	0,5643
p-value							0,7833	0,4
AR								
r							1	0,6669
p-value								0,2667

4.8 Survival analysis: Kaplan-Meier curves

To analyse the influence of the biomarkers expression on the overall survival, the patients were stratified in groups according to the median of the biomarkers expression as a cut-off.

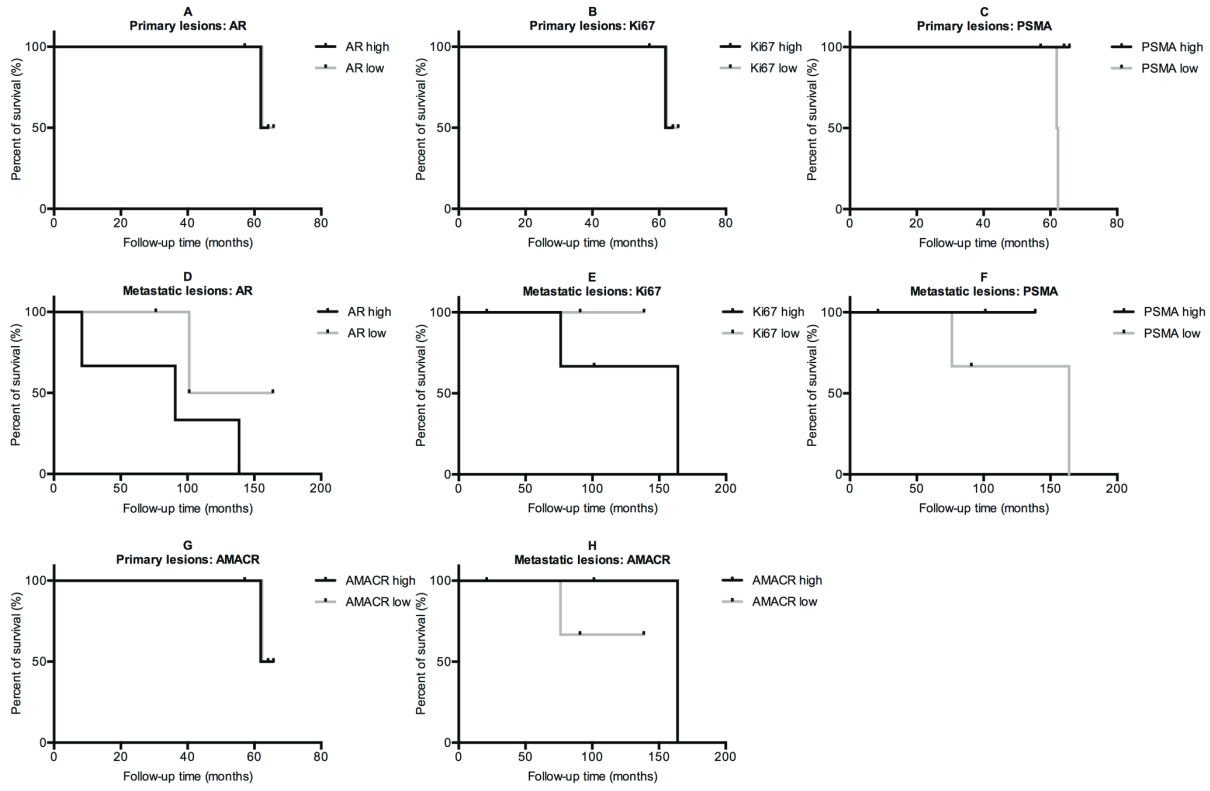

Figure 4.15. Analysis of the influence of the biomarkers expression in the survival of the patients for the primary and metastasis lesions. Kaplan-Meier curves of the primary lesions (n=5) of five patients, stratified by the percentage of biomarker expression: (A) AR, (B) Ki-67, (C) PSMA, (G) AMACR; and metastatic lesions (n=6) of five patients, also stratified by the percentage of

biomarker expression: (D) AR, (E) Ki-67, (F) PSMA, (H) AMACR. A median-based threshold was used to stratify the patient's samples in all analysis.

This resulted in a division of high and low expression groups for all markers, and a following analysis of the percentage of survival with the construction of Kaplan-Meier survival curves.

Figure 4.15 presents the Kaplan-Meier curves for all patients primary and metastasis lesions, stratified by biomarker expression levels. Neither the primary nor the metastasis survival curves exhibited statistical significance, based on the Mantel-Cox test.

As for the clinical variables, the same type of analysis was performed with data from the clinical TNM state, Gleason score, iPSA and first metastasis site (supplementary data: Figure 8.6). As expected, iPSA (Figure 4.14B) was significantly correlated with overall survival. Patients belonging to the group that was diagnosed with an initial PSA between 10 and 20 ng/mL (n=2) were associated with shorter survival times.

5 DISCUSSION

5.1 Clinico-pathological characteristics, the impact of metastasis site and molecular phenotype of primary samples

At diagnosis, the eight patients included in the multiplex IF study presented with a mean age of 61,9 years, a mean PSA of 11,3 ng/mL (Table 4.1), and most of them were diagnosed with a T2 stage.

According to a recent study about the preferable distribution of metastasis in PCa patients, the most common site for metastasis is the bone, followed by the LNs.[108] Conversely, in the whole cohort of 29 OM-PCa patients, identified at the Fundação Champalimaud, the most common metastasis site was the LNs, followed by bone, lung, brain and one case of suprarenal gland metastasis (supplementary data: Figure 8.1), this latter considered an atypical metastasis. The impact of the metastasis site in the patient's prognosis and probability of survival has received growing importance. In fact, by comparing the progression of patient 10 and 20, both presented an initial PSA level of 20 ng/mL, and likewise, both received HT as the first treatment, we can conclude that their tumors responded differently, resulting in different outcomes. Patient 10 experienced a quicker progression, presenting bone metastasis, and receiving SDRT as second treatment. Still, the tumors did not respond to treatment and the patient suffered bone and brain progression, and underwent more RT treatments that did not showed success, resulting in death. On the other hand, patient 20 had LN spread as first metastasis lesion, that were treated with SDRT. Similarly, also experienced bone progression, but underwent HT therapy and is currently alive with disease. In terms of the biomarkers expression in the biopsy samples, both showed no expression of Ki-67, AR and PSMA were overexpressed in 20B, and in contrast, PSMA was null in 10B (Figure 4.5). Given that, we would expect the molecular phenotype of the 20B case to correspond to a more aggressive tumor due to the AR overexpression, thus a worse prognostic for the patient. However, it all comes to the different first site of metastasis between the patients, and some studies believe that patients whose first metastasis lesions are to the bone (patient 10) have higher probability of disease progression and less survival rates, in contrast to LN as the first metastatic site. Patient 23 and 29 are very similar cases, presenting molecular phenotypes of the biopsies incredibly alike, as well as the PSA level at diagnosis. Both had LN progression that was treated with RT, and are currently in a NED state.

5.2 PSMA expression and PCa tumors heterogeneity

The incorporation of the membrane expressed protein PSMA in the multiplex IF improved the protocol and added additional data to compare the samples' phenotypes and perceive the great tissue heterogeneity of prostate cancers.

5.2.1 PSMA expression other than prostate cancer

PSMA is expressed by other cell types that can also be found in sectioned tissues of several organs, namely endothelial cells that constitute the blood vessels. This must be considered when analysing the expression of this protein in the tumor of tissues with high vasculature, such as the suprarenal gland metastasis.

5.2.2 The clinical potential of PSMA

A study that analysed the expression of PSMA and how it could be a potential clinical utility in the setting of high-risk PCa treatments[84], showed that PSMA varied considerably between adenocarcinomas localized in the prostate, LN metastasis and distant metastasis. PSMA was highly overexpressed in the LN metastasis, but lowered the expression levels when analysed in distant metastasis specimens, which was partially seen for the analysed cases in this project. PSMA did increase

from the primary localized tumors to the metastasis (Figure 4.8), although in a non-significant way. The metastasis that showed the highest PSMA levels were, indeed, the LNs (18M1, 29M), apart from the 22M. The distant metastasis from the adrenal gland and bone showed less expression when compared to the LNs. And, interestingly, we see in the metastasis progression of patient 18, a significant decrease from the LN to the distant bone metastasis, 18M2 (Figure 4.9A). Likewise, in patient 29's tumor progression, the PSMA overexpression in the LN metastasis, posterior to the prostate confined adenocarcinoma, presented elevated significance (Figure 4.9C).

On the other hand, because the late patients (10, 22, 27) expressed very low levels of PSMA in the analysed samples, low PSMA expression almost showed a significant association with shorter survival in the Kaplan-Meier analysis (Figure 4.15), contrary to what would be expected and what has been said about the potential of PSMA as a biomarker for high-risk PCa when overexpressed.

5.3 Comparison between the phenotypes of all samples of alive vs deceased patients

The evaluation of the mean biomarkers values for all primary and metastasis samples (Figure 4.8) showed no significant differences between the percentage of PSMA, AMACR, AR or Ki-67 expression levels between patients who are alive and deceased ones. Nevertheless, it's clear that Ki-67 is overexpressed in the metastatic sites (Figure 4.8, Figure 4.6 and Table 4.4). The isolated samples analysis allowed a well-defined graphical visualization of the phenotype and characteristic biomarker expression for each patient (Figure 4.5 and Figure 4.6). Noticeably, Figure 4.6 and the representative IF images (Figure 4.10) display how the metastasis samples phenotypes are much more heterogeneous than the primary biopsies, considering how many biomarkers were expressed in the tissue and the greater variance in percentage of expression.

5.3.1 Significant differences in the biomarkers expression levels between time-spaced biopsies

Although the mean samples' data of the primary and metastasis sites showed no significant differences for all markers, the opposite was seen for some markers when the analysed data was of the tumor progression samples, 18M1 – 18M2, 22B – 22M and 29P – 29M (Figure 4.9). We were expecting this kind of results by compressing all the data of all primaries samples, since this type of cancer shows great heterogeneity in all the expressed markers. Moreover, in all these, Ki-67 showed an interesting increased in time, statistically significant in all comparisons performed, suggesting that this marker may be associated with the progression of the tumors and the acquisition of a more aggressive phenotype. Ki-67 is highly associated with worse prognosis and, as so, percentages of expression higher than 3% are enough to classify a prostate tumor as highly proliferative. This biomarker raise is an important feature and may be used to predicting tumor progression, aiding tumor management and treatment.

The other markers, PSMA and AMACR, were also found with significant differences between samples, but there was no real association found, since none of them was found neither augmented nor diminished from the first sample to the second. For instance, PSMA decreased its expression in patient 18 (Figure 4.9A) and increased in patient 29 (Figure 4.9C), and AMACR increased in both of these patients and decreased drastically in patient 22 (Figure 4.9B). The alterations in the AR, interestingly, were always non-significant between samples.

Patients 18 and 22 underwent hormonal, chemo and radiotherapy, namely SDRT, as management treatments (Figure 4.11 and Figure 4.12). Patient 29, on the other hand, was treated exclusively with SDRT for all his metastatic lesions (Figure 4.13), and has shown a complete tumor response, being currently in a NED state, no evidence of disease, which can give some insight into the advantages of RT in controlling OM-PCa.

5.3.2 Phenotypes of the deceased patients

Another interesting difference is that by comparing patient number 22, deceased, with the others, we could see that the metastasis 22M suffered a lowering of all expressed markers, AMACR and AR, except for Ki-67, which presented a mean percentage of expression of 26%, value much higher than the other metastasis. Indeed, when looking at the molecular metastatic phenotypes of the deceased patients, namely 22M and 27M, the Ki-67 showed its higher expression levels. Again, this suggests that elevated Ki-67 expression in PCa dictates a true aggressive phenotype (Figure 4.6). Moreover, these patients presented similar clinical progression, with identical iPSA values, both had LN and bone metastization, in that order, and underwent SDRT, ineffectively, evolving with brain metastasis.

5.4 Biomarker AR expression: nuclei vs cytoplasm

Samples 18M1, 22M and 29M showed that AR was expressed both in the cytoplasm and nucleus of the cell, which may mean that the hormonal treatments, for patient 18 and 22, were showing some results, because the AR was being retained in the cytoplasm. This also suggests that these patients probably would not have great amount of the AR variants, e.g. AR-V7, that lead to CRPC and resistance to HT, but, nevertheless, patient 22 suffered a severe relapse. Thus, nucleus-only expression of the AR protein should be carefully addressed as a marker of tumor aggressiveness and progression to a CRPC state, having consequences in the subsequent course of treatment.

In addition, these samples presented high Ki-67 values, and Ki-67 and AR were found in many cases to be co-expressed in the nucleus, disputing the idea that cells in division would not have the AR activated and expressed in the nucleus.

5.5 Ki-67 and lack of a consistently defined threshold

Choosing the cut-off points for the biomarkers expression is a difficult task, but the median expression of a group of samples is used when a specific cut-off is not well documented. Meanwhile, cut-offs are being suggested for some biomarkers.[109] Regarding the choice for Ki-67 cut-off points, little consensus has been seen. The use of Ki-67 as a predictor of progression and disease-specific survival for PCa have long been debated, but the stratifications have been based on a wide range from 2.4% to 26%[110]. A recent paper by Fisher at al[111], reported the amazing potential of Ki-67 as an useful prognostic tool for patient diagnosis and management. They used a single biomarker, Ki-67, to predict a patient outcome based on first diagnosis specimens, and used a 10% cut-off for Ki-67 expression in these tissues. Others[110,112] have shown how higher Ki-67 expression can be predictive of increased risk of metastasis and reduced survival. By stratifying our samples with a cut-off 10% Ki-67 expression we got similar results to the median, where all primary specimens belonged to the low expressing group, which present values lower that 10%, and even lower than 5%, while all metastatic tissues presented values much higher than 10%, apart from 18M1 and 29M. Therefore, in this series of cases, there is no means of using Ki-67 as a marker of aggressiveness for an initial stage disease, since all our primary lesions would have fallen in the low-risk group.

5.6 Importance of nPSA and variations of the PSA level following treatment

The nPSA is an important tool used for PCa management. As previously mentioned, it can have different uses for treatment success and disease-free status, depending on the treatment, either surgery, RT or HT. Indeed, in the timeline for patients 18, 22 and 29 (Figure 4.11, Figure 4.12 and Figure 4.13, respectively) we can see the interesting variation of the PSA levels following the respective treatments. And for all patients its clear where the nPSA reaching takes place, in different time points for different therapies, and posteriorly, the rise in the PSA that preceded biochemical recurrence and that is used by the clinicians for patient management.

5.7 PSA expression and AR gene activity

Almost, if not all, of PCa patients are treated with HT at some point, and almost all present elevated levels of AR expression, which is associated with a reduced response to HT and a shorter relapse time, consequently promoting tumor growth and metastasis.[45,96] Also associated with the AR expression levels is the PSA blood levels, since the latter is regulated by the AR gene activity. Which hinted as to the utility of using both markers combined as a prediction tool for outcome.[45] However, in Figure 4.14A we got that the iPSA was negatively correlated with the AR expression levels on the primary lesions. This was an interesting result, and contrary to what was expected, because high PSA and AR levels are associated with more aggressive cancers and, as so, worse prognosis for the patients. Conversely, this result can be explained by the small sample size used for the correlation, because AR was mostly overexpressed across all samples, but for two patients, this overexpression coincided with low PSA at diagnosis.

5.8 Survival curves analysis

The Kaplan-Meier survival curves results were very thought-provoking despite not being statistically significant, probably again due to the sample size. But in Figure 4.15, it's clear that there is a difference in the survival curves from the primary lesions to the metastatic state, where in the latter it's possible to see the beginning of some interesting stratification of survival. It's remarkable how patients belonging to the low expressing groups for the AR and Ki-67 markers show 50 and 100% survival, respectively. Nonetheless, the only result that showed significance was with the iPSA stratification (Figure 4.14B), which was expected having in mind that only two patients were diagnosed with levels higher than 20 ng/mL, and from these only one is deceased. Furthermore, the two patients that presented iPSA between 10 and 20 ng/mL, are both dead. However, as previously said, the use of the PSA test as a diagnosis tool and management tool for PCa has been the target of controversy, for it doesn't present a reliable result. For example, the patients number 18, 23 and 29, all had relatively low initial PSA levels, but they are all also still alive with disease.

5.9 Challenges of multiplexed IF and image analysis

5.9.1 Software for bioimaging analysis

One of the most challenging things that must be optimized for this project is the image analysis part. Finding appropriate and capable software that allows the use of all the molecular data that the multiplex images hold, has shown to be a difficult task. It's not easy to classify protein markers that are co-localized, i.e. that are expressed in the same sub-cellular compartments, such as what happened with AR and AMACR, AR and Ki-67, and all the cytoplasmic ones with CK18, used for structural purposes. Thus, it is highly demanding to analyse images with five markers without resorting to the visualization of the isolated spectra images, and performing the analysis individually. Moreover, from all the software's tested for multiplex image analysis, which included inForm, ImageJ and QuPath, QuPath showed to be the most versatile and easy-to-use, presenting tools for a flexible quantification of the biomarkers, either automatically, manually or both. The trial with the inForm software revealed the promising use of interesting tools such as the tissue and cell/object segmentation, as well as, the cell phenotyping. Although very promising, these tools didn't work in the complex multiplexed context of our images, majorly because they allow the assignment of only one "phenotype" to a single cell, so a cell could not be AR and Ki-67 positive, or AMACR and AR positive, which was a dead-end for performing image analysis. Nevertheless, the tissue segmentation followed by cell count gives interesting results comparing tumor versus stroma/normal tissue.

5.9.2 Challenges of IF and multiplex IHC

Other difficulties were encountered as the IF scanned images were themselves analysed. Namely, the loss of DAPI in a lot of images (which can be seen in some representative IF images, e.g. Figure 4.10A, 18M1), and how to find the perfect isolated spectra for the multispectral unmixing. This loss of DAPI was mostly seen whenever the AR was overexpressed in the nuclei, and whenever the malignant nuclei were displayed as a hollow, characteristic of prostate tumor cells. To partially solve the DAPI staining complication, two different multispectral libraries were built, one for a DAPI faint counter-stain and another for a strong DAPI, decision made after the scanning process was done. Also, for some reason, in some cases, DAPI would lose its proprieties and the nuclei would appear coloured in faint orange. We have no real explanation for this strange process, but some ideas were that it could be due to the prolonged light exposure of the stained tissue, or perhaps from the last fixation step of the protocol, that consisted in a 10% formalin dip. Still, whenever the microscope visualization showed the orange nuclei, a vigorous washing step was performed, followed by another mounting with DAPI to overcome this problem.

5.9.3 Multispectral library building

As previously mentioned, we used double-plex and single-plex stained slides to build the multispectral library. Unfortunately, we didn't get the results we were expecting, which were a clearer spectra library with less background noise. Instead, we got unmixed images with no signal or unspecific signal for some of the antibodies, and significant differences in the background in the different analysed tissues. We couldn't figure out why the library wasn't working properly, and why the software wasn't able to successfully isolate the spectra corresponding to the pure antibody in the multiplex images, but we think it could be due to the great spectra complexity of the 5-plex staining, and the sub-cellular co-localization of some antibodies. Antibodies that are present in the same sub-cellular component are difficult to differentiate, especially when the emission spectra of the labelled secondary antibodies have a very close peak in the emission spectrum, such as what we have with AR and AMACR (Figure 4.2). In our experience, building a library from the multiplex stained slide gives much better results for the analyses than using single and double-plex.

Nevertheless, the potential of the multiplex IF technique in research is vast, for it acknowledges multidimensional data related to tissue architecture, spatial distribution of multiple cell phenotypes, co-expression of signalling and cell cycle markers.

5.10 Nucleic acid extraction from FFPE slides, sequencing and future perspectives

The future step in the project consists in using the extracted nucleic acids from these samples and perform targeted sequencing using the Oncomine® Comprehensive Assay kit with the Ion Torrent™ System (ThermoFisher Scientific, Waltham, MA), which interrogates the most commonly altered 143 cancer genes (73 oncogenes, 49 copy number altered genes, 26 tumor suppressors genes and 22 fusion driver genes), including the AR gene. The results from the sequencing will add molecular data to the project and, together with the molecular phenotypes analysed, will give some insight into the differences in tumor responses between patients, predominantly why some cases that are similar phenotypically behave differently and lead to distinctive outcomes. Besides this, cfDNA isolated from blood extracted at several time-points would be an interesting addition, exploring the liquid biopsy concept, by tracking changes in the DNA during the natural course of the disease, and possibly predicting the response to treatments.

6 CONCLUSIONS

The molecular phenotyping and data analysis obtained by multiplex IF quantitative biomarker expression levels with multispectral microscopy allowed a comparison between different phenotypes and clinico-pathological characteristics of eight patients with OM-PCa. Multiplex assays for several biomarkers on tissue sections are not very common, mainly because of technical issues regarding the use of multiple IFs, different tissues reactions and image analysis. Nevertheless, multiplex IF allowed the obtainment a great amount of molecular data from a single stained tissue slide.

Our experiments identified a possible aggressive molecular phenotype, associated with a worse disease scenario and shorter recurrent-free survival, presented with high expression of AR, Ki-67 and possibly AMACR and PSMA, although these latter are very heterogeneously expressed along metastatic samples. The loss of expression of biomarkers such as AR and PSMA was also a sign of progression and led to treatment unresponsiveness, as seen in the metastatic progression of two of our patients. Instead, a potentially curable OM-PCa molecular phenotype would present a not too high AR expression (less than around 50%) and a Ki-67 level of expression below 10%. After all, patients that exhibited a metastatic overexpression of this marker (higher than 20%) did not respond to therapy and RT treatments showed little probability of success in controlling the tumors. Hence, when analysing metastasis samples of OM-PCa we suggest using a cut-off of 20% for Ki-67. Interestingly, there is a patient in this group of patients who was treated exclusively with SDRT for all his metastatic lesions and has shown a complete tumor response, being alive with no evidence of disease at follow-up. This, together with the phenotyping of his samples, suggests that he may be an example of a “true” oligometastatic patient.

In conclusion, using a molecular phenotyping of PCa specimens with a multiplexed biomarkers quantification approach might provide some insight of each individual’s tumor behaviour and, consequently, aid their clinical management, aiming for a successful course of treatment for complete recovery and/or longer recurrent-free survival.

7 References

1. Siegel RL, Miller KD, Jemal A. Cancer statistics. *CA Cancer J Clin*. 2016;66(1):7-30. doi:10.3322/caac.21332.
2. Ferlay J, Steliarova-Foucher E, Lortet-Tieulent J, et al. Cancer incidence and mortality patterns in Europe: Estimates for 40 countries in 2012. *Eur J Cancer*. 2013;49(6):1374-1403. doi:10.1016/j.ejca.2012.12.027.
3. Ellis, Leight; Lehet, Kristin; Ramakrishnan, Swathi; Adelaiye, Remi; Pili R. Development of a Castrate Resistant Transplant Tumor Model of Prostate Cancer. *Prostate*. 2008;144(5):724-732. doi:10.1038/jid.2014.371.
4. Attard G, Parker C, Eeles RA, et al. Prostate cancer. *Lancet*. 2016;387(10013):70-82. doi:10.1016/S0140-6736(14)61947-4.
5. Verze P, Cai T, Lorenzetti S. The role of the prostate in male fertility, health and disease. *Nat Rev Urol*. 2016. doi:10.1038/nrurol.2016.89.
6. Epperson J, Frank WL. Male genital cancers. *Prim Care - Clin Off Pract*. 1998;25(2):459. doi:10.1016/S0095-4543(05)70076-2.
7. Okada H, Tsubura A, Okamura A, et al. Keratin profiles in normal/hyperplastic prostates and prostate carcinoma. *Virchows Arch A Pathol Anat Histopathol*. 1992;421(2):157-161. doi:10.1007/BF01607049.
8. Moscatelli D, Wilson EL. PINing Down the Origin of Prostate Cancer. *Sci Transl Med*. 2010;2(43):43ps38-43ps38. doi:10.1126/scitranslmed.3001445.
9. Meilhac S, Zaffran S, Kirby ML, et al. Identification of a Cell of Origin. *Science (80-)*. 2010;(July):568-571.
10. Epstein JI, Allsbrook Jr WC, Amin MB, Egevad LL and the IGC. The 2005 International Society of Urological Pathology (ISUP) Consensus Conference on Glea- son Grading of Prostatic Carcinoma. *Eur Urol*. 2006;49(4):757-758. doi:10.1016/j.eururo.2006.02.006.
11. Gleason DF. Histologic grading of prostate cancer: A perspective. *Hum Pathol*. 1992;23(3):273-279. doi:10.1016/0046-8177(92)90108-F.
12. Pierorazio PM, Walsh PC, Partin AW, Epstein JI. Prognostic Gleason grade grouping: Data based on the modified Gleason scoring system. *BJU Int*. 2013;111(5):753-760. doi:10.1111/j.1464-410X.2012.11611.x.
13. Brawer MK. Prostatic intraepithelial neoplasia: A premalignant lesion. *J Cell Biochem*. 1992;50(S16G):171-174. doi:10.1002/jcb.240501129.
14. Bostwick DG. High grade prostatic intraepithelial neoplasia. The most likely precursor of prostate cancer. *Cancer*. 1995;75(S7):1823-1836. doi:10.1002/1097-0142(19950401)75:7+<1823::AID-CNCR2820751612>3.0.CO;2-7.
15. Bostwick DG, Pacelli A, Lopez-Beltran A. Molecular biology of prostatic intraepithelial neoplasia. *Prostate*. 1996;29(I 996):117-134. doi:10.1002/(SICI)1097-0045(199608)29:2<117::AID-PROS7>3.0.CO;2-C.
16. Bracarda S, De Cobelli O, Greco C, et al. Cancer of the prostate. *Crit Rev Oncol Hematol*. 2005;56(3):379-396. doi:10.1016/j.critrevonc.2005.03.010.
17. Heidenreich A, Bellmunt J, Bolla M, et al. EAU guidelines on prostate cancer. Part 1: Screening, diagnosis, and treatment of clinically localised disease. *Eur Urol*. 2011;59(1):61-71. doi:10.1016/j.eururo.2010.10.039.
18. Damber J-E, Aus G. Prostate cancer. *Lancet*. 2008;371(9625):1710-1721. doi:10.1016/S0140-6736(08)60729-1.
19. Tomlins S a, Rhodes DR, Perner S, et al. Recurrent Fusion of TMPRSS2 and ETC Transcription Factor Genes in Prostate Cancer. *Science (80-)*. 2005;310(October):644-648. doi:10.1126/science.1117679.
20. Abeshouse A, Ahn J, Akbani R, et al. The Molecular Taxonomy of Primary Prostate Cancer. *Cell*. 2015;163(4). doi:10.1016/j.cell.2015.10.025.
21. Visakorpi T, Hyytinen E, Koivisto P, et al. In vivo amplification of the androgen receptor gene and progression of human prostate cancer. *Nat Genet*. 1995;9(4):401-406. http://dx.doi.org/10.1038/ng0495-401.
22. Barbieri CE, Baca SC, Lawrence MS, et al. Exome sequencing identifies recurrent SPOP , FOXA1 and

MED12 mutations in prostate cancer. *Nat Genet*. 2012;44(6):685-689. doi:10.1038/ng.2279.
23. Tomlins SA, Bjartell A, Chinnaiyan AM, et al. ETS Gene Fusions in Prostate Cancer: From Discovery to Daily Clinical Practice. *Eur Urol*. 2009;56(2):275-286. doi:10.1016/j.eururo.2009.04.036.
24. Spratt DE, Zumsteg ZS, Feng FY, Tomlins SA. Translational and clinical implications of the genetic landscape of prostate cancer. *Nat Rev Clin Oncol*. 2016. doi:10.1038/nrclinonc.2016.76.
25. Pritchard CC, Mateo J, Walsh MF, et al. Inherited DNA-Repair Gene Mutations in Men with Metastatic Prostate Cancer. *N Engl J Med*. 2016;375(5):443-453. doi:10.1056/NEJMoa1603144.
26. Taylor RA, Fraser M, Livingstone J, et al. Germline BRCA2 mutations drive prostate cancers with distinct evolutionary trajectories. *Nat Commun*. 2017;8:13671. doi:10.1038/ncomms13671.
27. Edwards SM, Kote-Jarai Z, Meitz J, et al. Two percent of men with early-onset prostate cancer harbor germline mutations in the BRCA2 gene. *Am J Hum Genet*. 2003;72(1):1-12.
28. Taylor BS, Schultz N, Hieronymus H, et al. Integrative Genomic Profiling of Human Prostate Cancer. *Cancer Cell*. 2010;18(1):11-22. doi:10.1016/j.ccr.2010.05.026.
29. Valdés-Mora F, Clark SJ. Prostate cancer epigenetic biomarkers: next-generation technologies. *Oncogene*. 2014. doi:10.1038/onc.2014.111.
30. Hernandez DJ, Nielsen ME, Han M, Partin AW. Contemporary Evaluation of the D'Amico Risk Classification of Prostate Cancer. *Urology*. 2007;70(5):931-935. doi:10.1016/j.urology.2007.08.055.
31. D'Amico A V, Whittington R, Malkowicz SB, et al. Biochemical outcome after radical prostatectomy, external beam radiation therapy, or interstitial radiation therapy for clinically localized prostate cancer. *JAMA*. 1998;280(11):969-974. http://www.ncbi.nlm.nih.gov/entrez/query.fcgi?cmd=Retrieve&db=PubMed&dopt=Citation&list_uids=9749478.
32. National Comprehensive Cancer Network. NCCN Clinical Practice Guidelines in Oncology (NCCN Guidelines (R)). 2017;Version I. doi:10.1016/S0140-6736(08)60729-1.
33. N. Mottet, J. Bellmunt, E. Briers , M. Bolla, P. Cornford, M. De Santis AH, S. Joniau, T. Lam, M.D. Mason, V. Matveev, H. van der Poel, T.H. van der Kwast, O. Rouvière TWGARCN van den B, T. van den Broeck, N.J. van Casteren, W. Everaerts, L. Marconi PM. *Guidelines on Prostate Cancer*. Vol 53.; 2016. doi:10.1016/j.eururo.2007.09.002.
34. Sobin L, Gospodarowicz M WC (eds). *TNM Classification of Malignant Tumours*. seventh. Wiley-BlackWell; 2009.
35. Stamey TA, Yang N, Hay AR, McNeal JE, Freiha FS, Redwine E. Prostate-specific antigen as a serum marker for adenocarcinoma of the prostate. *N Engl J Med*. 1987;317(15):909-916. doi:10.1056/NEJM198710083171501.
36. Leman ES, Getzenberg RH. Biomarkers for prostate cancer. *J Cell Biochem*. 2009;108(1):3-9. doi:10.1002/jcb.22227.
37. Prensner JR, Rubin MA, Wei JT, Chinnaiyan AM. Beyond PSA: the next generation of prostate cancer biomarkers. *Sci Transl Med*. 2012;4(127):127rv3. doi:10.1126/scitranslmed.3003180.
38. Bickers B, Aukim-Hastie C. New molecular biomarkers for the prognosis and management of prostate cancer--the post PSA era. *Anticancer Res*. 2009;29(8):3289-3298. http://www.ncbi.nlm.nih.gov/pubmed/19661347.
39. Nadler RB, Humphrey P a, Smith DS, Catalona WJ, Ratliff TL. Effect of inflammation and benign prostatic hyperplasia on elevated serum prostate specific antigen levels. *J Urol*. 1995;154(2):407-413. doi:10.1016/S0022-5347(01)67064-2.
40. Goonewardene SS, Phull JS, Bahl A, Persad RA. Interpretation of PSA levels after radical therapy for prostate cancer. *Trends Urol Men's Heal*. 2014;5(4):30-34. http://10.0.3.234/tre.407%0Ahttp://search.ebscohost.com/login.aspx?direct=true&db=a9h&AN=97193612&site=ehost-live.
41. Humphreys EB, Mangold LA, Eisenberger M, Dorey FJ, Walsh PC, Partin AW. Risk of Prostate Cancer–Specific Mortality Following Biochemical Recurrence After Radical Prostatectomy. *JAMA*. 2005;294(4):433-439.
42. Critz FA, Levinson AK, Williams WH, Holladay DA, Holladay CT. The PSA nadir that indicates potential cure after radiotherapy for prostate cancer. *Urology*. 1997;49(3):322-326. doi:10.1016/S0090-4295(96)00666-8.

43. Kwak C, Jeong SJ, Park MS, Lee E, Lee SE. Prognostic significance of the nadir prostate specific antigen level after hormone therapy for prostate cancer. *J Urol*. 2002;168(3):995-1000. doi:10.1097/01.ju.0000024925.67014.21.
44. Heidenreich A, Bastian PJ, Bellmunt J, et al. EAU guidelines on prostate cancer. Part II: Treatment of advanced, relapsing, and castration-resistant prostate cancer. *Eur Urol*. 2014;65(2):467-479. doi:10.1016/j.eururo.2013.11.002.
45. Donovan MJ, Osman I, Khan FM, et al. Androgen receptor expression is associated with prostate cancer-specific survival in castrate patients with metastatic disease. *BJU Int*. 2010;105(4):462-467. doi:10.1111/j.1464-410X.2009.08747.x.
46. Barker HE, Paget JTE, Khan AA, Harrington KJ. The tumour microenvironment after radiotherapy: mechanisms of resistance and recurrence. *Nat Rev Cancer*. 2015;15(7):409-425. doi:10.1038/nrc3958.
47. Delaney G, Jacob S, Featherstone C, Barton M. The role of radiotherapy in cancer treatment: Estimating optimal utilization from a review of evidence-based clinical guidelines. *Cancer*. 2005;104(6):1129-1137. doi:10.1002/cncr.21324.
48. Barnett GC, West CML, Dunning AM, et al. Normal tissue reactions to radiotherapy: towards tailoring treatment dose by genotype. *Nat Rev Cancer*. 2009;9(2):134-142. doi:10.1038/nrc2587.
49. Baumann M, Krause M, Overgaard J, et al. Radiation oncology in the era of precision medicine. *Nat Rev Cancer*. 2016;16(4):234-249. doi:10.1038/nrc.2016.18.
50. Arcangeli S, Greco C. Hypofractionated radiotherapy for organ-confined prostate cancer: is less more? *Nat Rev Urol*. 2016;13(7):400-408. doi:10.1038/nrurol.2016.106.
51. Zelefsky MJ, Greco C, Motzer R, et al. Tumor control outcomes after hypofractionated and single-dose stereotactic image-guided intensity-modulated radiotherapy for extracranial metastases from renal cell carcinoma. *Int J Radiat Oncol Biol Phys*. 2012;82(5):1744-1748. doi:10.1016/j.ijrobp.2011.02.040.
52. Greco C, Pares O, Pimentel N, et al. Spinal metastases: From conventional fractionated radiotherapy to single-dose SBRT. *Reports Pract Oncol Radiother*. 2015;20(6):454-463. doi:10.1016/j.rpor.2015.03.004.
53. Laliscia C, Fabrini MG, Delishaj D, et al. Clinical Outcomes of Stereotactic Body Radiotherapy in Oligometastatic Gynecological Cancer. *Int J Gynecol Cancer*. 2017;27(2):396-402. doi:10.1097/IGC.0000000000000885.
54. Conde Moreno AJ, Ferrer Albiach C, Muelas Soria R, González Vidal V, García Gómez R, Albert Antequera M. Oligometastases in prostate cancer: restaging stage IV cancers and new radiotherapy options. *Radiat Oncol*. 2014;9:258. doi:10.1186/s13014-014-0258-7.
55. Hanahan D, Weinberg RA. Hallmarks of cancer: The next generation. *Cell*. 2011;144(5):646-674. doi:10.1016/j.cell.2011.02.013.
56. Mehlen P, Puisieux A. Metastasis: a question of life or death. *Nat Rev Cancer*. 2006;6(6):449-458. doi:10.1038/nrc1886.
57. Steeg PS. Targeting metastasis. *Nat Rev Cancer*. 2016;16(4):201-218. doi:10.1038/nrc.2016.25.
58. Gupta GP, Massagué J. Cancer Metastasis: Building a Framework. *Cell*. 2006;127(4):679-695. doi:10.1016/j.cell.2006.11.001.
59. Hellman, S., Weichselbaum RR. Oligometastases. *J Clin Oncol*. 1995;13(1):8-10.
60. Tosoian JJ, Gorin MA, Ross AE, Pienta KJ, Tran PT, Schaeffer EM. Oligometastatic prostate cancer: definitions, clinical outcomes, and treatment considerations. *Nat Rev Urol*. 2016. doi:10.1038/nrurol.2016.175.
61. Lussier YA, Xing HR, Salama JK, et al. Microrna expression characterizes Oligometastasis(es). *PLoS One*. 2011;6(12). doi:10.1371/journal.pone.0028650.
62. Schaeffer CW, Partin AW, Isaacs WB, Coffey DS, Isaacs JT. Molecular and cellular changes associated with the acquisition of metastatic ability by prostatic cancer cells. *Prostate*. 1994;25:249-265.
63. Stevens DJ, Sooriakumaran P. Oligometastatic Prostate Cancer. *Curr Treat Options Oncol*. 2016;17(12). doi:10.1007/s11864-016-0439-8.
64. McDunn JE, Li Z, Adam KP, et al. Metabolomic signatures of aggressive prostate cancer. *Prostate*. 2013. doi:10.1002/pros.22704.
65. Prensner JR, Zhao S, Erho N, et al. RNA biomarkers associated with metastatic progression in prostate cancer: A multi-institutional high-throughput analysis of SChLAP1. *Lancet Oncol*. 2014;15(13):1469-1480. doi:10.1016/S1470-2045(14)71113-1.

66. Endzeliņš E, Melne V, Kalniņa Z, et al. Diagnostic, prognostic and predictive value of cell-free miRNAs in prostate cancer: a systematic review. *Mol Cancer*. 2016;15(1):41. doi:10.1186/s12943-016-0523-5.
67. Guo H, Ahmed M, Zhang F, et al. Modulation of long noncoding RNAs by risk SNPs underlying genetic predispositions to prostate cancer. *Nat Genet*. 2016;(August):1-12. doi:10.1038/ng.3637.
68. Fabris L, Ceder Y, Chinnaiyan AM, et al. The Potential of MicroRNAs as Prostate Cancer Biomarkers. *Eur Urol*. 2016;70(2):312-322. doi:10.1016/j.eururo.2015.12.054.
69. Luo J, Zha S, Gage WR, et al. Alpha-methylacyl-CoA racemase: a new molecular marker for prostate cancer. *Cancer Res*. 2002;62:2220-2226.
70. Rubin MA, Zhou M, Dhanasekaran SM, et al. α-Methylacyl Coenzyme A Racemase as a Tissue Biomarker for Prostate Cancer. *JAMA*. 2002;287(13):1662. doi:10.1001/jama.287.13.1662.
71. Jiang N, Zhu S, Chen J, Niu Y, Zhou L. A-Methylacyl-CoA Racemase (AMACR) and Prostate-Cancer Risk: A Meta-Analysis of 4,385 Participants. *PLoS One*. 2013;8(10):1-6. doi:10.1371/journal.pone.0074386.
72. Alinezhad S, Väänänen R-M, Ochoa NT, et al. Global expression of AMACR transcripts predicts risk for prostate cancer - a systematic comparison of AMACR protein and mRNA expression in cancerous and noncancerous prostate. *BMC Urol*. 2016;16:10. doi:10.1186/s12894-016-0128-8.
73. Taplin M, Bubley GJ, Ko Y, et al. Selection for Androgen Receptor Mutations in Prostate Cancers Treated with Androgen Antagonist. *Cancer Res*. 1999;59(11):2511-2515.
74. Craft N, Shostak Y, Carey M, Sawyers CL. A mechanism for hormone-independent prostate cancer through modulation of androgen receptor signaling by the HER-2/neu tyrosine kinase. *Nat Med*. 1999;5(3):280-285. doi:10.1038/6495.
75. Zhang X, Morrissey C, Sun S, et al. Androgen receptor variants occur frequently in castration resistant prostate cancer metastases. *PLoS One*. 2011;6(11). doi:10.1371/journal.pone.0027970.
76. Scher HI, Sawyers CL. Biology of progressive, castration-resistant prostate cancer: Directed therapies targeting the androgen-receptor signaling axis. *J Clin Oncol*. 2005;23(32):8253-8261. doi:10.1200/JCO.2005.03.4777.
77. Weng H, Li S, Huang J-Y, et al. Androgen receptor gene polymorphisms and risk of prostate cancer: a meta-analysis. *Sci Rep*. 2017;7(June 2016):40554. doi:10.1038/srep40554.
78. Azad AA, Volik S V., Wyatt AW, et al. Androgen receptor gene aberrations in circulating cell-free DNA: Biomarkers of therapeutic resistance in castration-resistant prostate cancer. *Clin Cancer Res*. 2015;21(10):2315-2324. doi:10.1158/1078-0432.CCR-14-2666.
79. Antonarakis ES, Lu C, Luber B, et al. Association Between Androgen Receptor Splice Variants and Prostate Cancer Resistance to Abiraterone and Enzalutamide. *J Clin Oncol*. 2017:JCO.2016.70.196. doi:10.1200/JCO.2016.70.1961.
80. Murphy GP, Barren RJ, Erickson SJ, et al. Evaluation and comparison of two new prostate carcinoma markers. Free-prostate specific antigen and prostate specific membrane antigen. *Cancer*. 1996;78(1):809-818. doi:10.1002/(SICI)1097-0142(19960815)78:4<809::AID-CNCR18>3.0.CO;2-Z.
81. Murphy GP, Tino WT, Holmes EH, et al. Measurement of prostate-specific membrane antigen in the serum with a new antibody. *Prostate*. 1996;28(4):266-271. doi:10.1002/(SICI)1097-0045(199604)28:4<266::AID-PROS7>3.0.CO;2-B.
82. Murphy GP, Greene TG, Tino WT, Boynton AL, Holmes EH. Isolation and characterization of monoclonal antibodies specific for the extracellular domain of prostate specific membrane antigen. *J Urol*. 1998;160(6 Pt 2):2396-2401. http://www.ncbi.nlm.nih.gov/pubmed/9817391.
83. Minner S, Wittmer C, Graefen M, et al. High level PSMA expression is associated with early psa recurrence in surgically treated prostate cancer. *Prostate*. 2011;71(3):281-288. doi:10.1002/pros.21241.
84. Perner S, Hofer MD, Kim R, et al. Prostate-specific membrane antigen expression as a predictor of prostate cancer progression. *Hum Pathol*. 2007;38(5):696-701. doi:10.1016/j.humpath.2006.11.012.
85. Ross JS, Sheehan CE, Fisher H a G, et al. Correlation of primary tumor prostate-specific membrane antigen expression with disease recurrence in prostate cancer. *Clin Cancer Res*. 2003;9(17):6357-6362. doi:10.1016/s0022-5347(01)62198-0.
86. Ben Jemaa A, Bouraoui Y, Sallami S, et al. Co-expression and impact of prostate specific membrane antigen and prostate specific antigen in prostatic pathologies. *J Exp Clin Cancer Res*. 2010;29(1):171. doi:10.1186/1756-9966-29-171.

87. Silver D, Pellicer I, Fair W, Heston W, Cordon-Cardo C. Prostate-specific Membrane Antigen Expression in Normal and Malignant Human Tissues. *Clin cancer Res*. 1997;3(January):81–85. http://clincancerres.aacrjournals.org/content/3/1/81.short.
88. Maurer T, Eiber M, Schwaiger M, Gschwend JE. Current use of PSMA–PET in prostate cancer management. *Nat Rev Urol*. 2016:1-10. doi:10.1038/nrurol.2016.26.
89. Haberkorn U, Eder M, Kopka K, Babich JW, Eisenhut M. New strategies in prostate cancer: Prostate-specific membrane antigen (PSMA) ligands for diagnosis and therapy. *Clin Cancer Res*. 2016;22(1):9-15. doi:10.1158/1078-0432.CCR-15-0820.
90. Costa J. Evidence-Based Pathology. *Int J Surg Pathol*. 2007;15(3):230-232.
91. Costa J. Systems medicine in oncology. *Nat Clin Pract Oncol*. 2008;5(3):117. doi:10.1038/ncponc1070.
92. Costa J. Is clinical systems pathology the future of pathology? *Arch Pathol Lab Med*. 2008;132(5):774-776. doi:10.1043/1543-2165(2008)132[774:ICSPTF]2.0.CO;2.
93. Saidi O, Cordon-Cardo C, Costa J. Technology insight: will systems pathology replace the pathologist? *Nat Clin Pract Urol*. 2007;4(1):39-45. doi:10.1038/ncpuro0669.
94. Carlos Cordon-Cardo, Angeliki Kotsianti, David A. Verbel MT, Paola Capodieci, Stefan Hamann, Yusuf Jeffers, Mark Clayton, Faysal Elkhettabi, Faisal M. Khan, Marina Sapir, Valentina Bayer-Zubek, Yevgen Vengrenyuk, Stephen Fogarsi, Olivier Saidi, Victor E. Reuter, Howard I. Scher, Michael W. and MJD. Improved prediction of prostate cancer recurrence through systems pathology. *J Clin Invest*. 2007;117(7):1-8. doi:10.1172/JCI31399DS1.
95. Donovan MJ, Costa J, Cordon-Cardo C. Systems pathology: A paradigm shift in the practice of diagnostic and predictive pathology. *Cancer*. 2009;115(SUPPL 13):3078-3084. doi:10.1002/cncr.24353.
96. Donovan MJ, Hamann S, Clayton M, et al. Systems pathology approach for the prediction of prostate cancer progression after radical prostatectomy. *J Clin Oncol*. 2008;26(24):3923-3929. doi:10.1200/JCO.2007.15.3155.
97. Donovan MJ, Khan FM, Bayer-Zubek V, Powell D, Costa J, Cordon-Cardo C. A systems-based modelling approach using transurethral resection of the prostate (TURP) specimens yielded incremental prognostic significance to Gleason when predicting long-term outcome in men with localized prostate cancer. *BJU Int*. 2012;109(2):207-213. doi:10.1111/j.1464-410X.2011.10316.x.
98. Jr LAD, Bardelli A, Diaz LA, Bardelli A. Liquid Biopsies: Genotyping Circulating Tumor DNA. *J Clin Oncol*. 2014;32(6):579-586. doi:10.1200/JCO.2012.45.2011.
99. Meo A Di, Bartlett J, Cheng Y, Pasic MD, Yousef GM. Liquid biopsy : a step forward towards precision medicine in urologic malignancies. *Mol Cancer*. 2017:1-14. doi:10.1186/s12943-017-0644-5.
100. Vaart M Van Der, Pretorius PJ. Circulating DNA Its Origin and Fluctuation. *New York Acad Sci*. 2008;27(0):18-26. doi:10.1196/annals.1448.022.
101. Schwarzenbach H, Hoon DSB, Pantel K. Cell-free nucleic acids as biomarkers in cancer patients. *Nat Rev Cancer*. 2011;11(6):426-437. doi:10.1038/nrc3066.
102. Crowley E, Nicolantonio F Di, Loupakis F, Bardelli A. Liquid biopsy: monitoring cancer-genetics in the blood. *Nat Rev Cancer*. 2013:13. doi:10.1038/nrclinonc.2013.110.
103. Breitbach S, Tug S, Helmig S, et al. Direct Quantification of Cell-Free , Circulating DNA from Unpurified Plasma. *PLoS One*. 2014;9(3):11. doi:10.1371/journal.pone.0087838.
104. Eliceiri KW, Berthold MR, Goldberg IG, et al. Biological imaging software tools. *Nat Methods*. 2012;9(7):697-710. doi:10.1038/nmeth.2084.
105. Cardona A, Tomancak P. Current challenges in open-source bioimage informatics. *Nat Methods*. 2012;9(7):661-665. doi:10.1038/nmeth.2082.
106. Bankhead P, Loughrey MB, Fernández JA, et al. QuPath : Open source software for digital pathology image analysis. 2017:1-27. doi:https://doi.org/10.1101/099796.
107. Stack EC, Wang C, Roman KA, Hoyt CC. Multiplexed immunohistochemistry, imaging, and quantitation: A review, with an assessment of Tyramide signal amplification, multispectral imaging and multiplex analysis. *Methods*. 2014;70(1):46-58. doi:10.1016/j.ymeth.2014.08.016.
108. Gandaglia G, Karakiewicz PI, Briganti A, et al. Impact of the Site of Metastases on Survival in Patients with Metastatic Prostate Cancer. *Eur Urol*. 2015;68(2):325-334. doi:10.1016/j.eururo.2014.07.020.
109. Barber AG, Castillo-Martin M, Bonal DM, Rybicki BA, Christiano AM, Cordon-Cardo C. Characterization of desmoglein expression in the normal prostatic gland. Desmoglein 2 is an independent

prognostic factor for aggressive prostate cancer. *PLoS One*. 2014;9(6). doi:10.1371/journal.pone.0098786.
110. Green WJF, Ball G, Hulman G, et al. KI67 and DLX2 predict increased risk of metastasis formation in prostate cancer – a targeted molecular approach. *J Clin Oncol*. 2016;115(2):236-242. doi:10.1038/bjc.2016.169.
111. Fisher G, Yang ZH, Kudahetti S, et al. Prognostic value of Ki-67 for prostate cancer death in a conservatively managed cohort. *BJU Int*. 2013;(September 2012):271-277. doi:10.1038/bjc.2012.598.
112. Group TO, Chase F, Health I, et al. MDM2 and Ki-67 Predict for Distant Metastasis and Mortality in Men Treated With Radiotherapy and Androgen Deprivation for Prostate Cancer : RTOG 92-02. *J Clin Oncol*. 2009;27(19):3177-3184. doi:10.1200/JCO.2008.19.8267.

8 Supplementary data

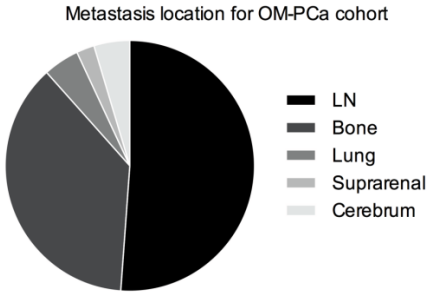

Figure 8.1. Pie chart for the location of the metastasis in the whole 29 OM-PCa patient cohort. LN – lymph node.

Patient sample: 10B					
ROIs analysed	5				
	# cells expressing				total # cells
	PSMA	AMACR	AR	KI67	DAPI
ROI 1	0	231	102	0	231
ROI 2	0	108	68	0	126
ROI 3	0	155	84	0	175
ROI 4	0	92	124	0	153
ROI 5	0	221	76	0	247
	% cells expressing:				
ROI 1	0	100	44,1558442	0	
ROI 2	0	85,7142857	53,968254	0	
ROI 3	0	88,5714286	48	0	
ROI 4	0	60,130719	81,0457516	0	
ROI 5	0	89,4736842	30,7692308	0	
MEAN	0	84,7780235	51,5878161	0	
SD	0	14,802989	18,5402035	0	

Patient sample: 20B					
ROIs analysed	3				
	# cells expressing				total # cells
	PSMA	AMACR	AR	KI67	DAPI
ROI 1	495	481	429	0	495
ROI 2	479	464	380	0	486
ROI 3	319	314	232	0	355
	% cells expressing:				
ROI 1	100	97,1717172	86,6666667	0	
ROI 2	98,5596708	95,473251	78,1893004	0	
ROI 3	89,8591549	88,4507042	65,3521127	0	
MEAN	96,1396086	93,6985575	76,7360266	0	
SD	5,48650258	4,62343699	10,7313353	0	

Patient sample: 22B					
ROIs analysed	6				
	# cells expressing				total # cells
	PSMA	AMACR	AR	KI67	DAPI
ROI 1	0	1681	1217	35	1739
ROI 2	0	1478	1166	20	1500
ROI 3	0	1902	1787	17	2029
ROI 4	0	1600	1145	42	1630
ROI 5	0	858	843	23	1060
ROI 6	0	1162	907	115	1189
	% cells expressing:				
ROI 1	0	96,665	69,983	2,013	
ROI 2	0	98,533	77,733	1,333	
ROI 3	0	93,741	88,073	0,838	
ROI 4	0	98,160	70,245	2,577	
ROI 5	0	80,943	79,528	2,170	
ROI 6	0	97,729	76,283	9,672	
MEAN	0,000	94,295	76,974	3,100	
SD	0	6,76579253	6,70697074	3,27874849	

Patient sample: 23B					
ROIs analysed	5				
	# cells expressing				total # cells
	PSMA	AMACR	AR	KI67	DAPI
ROI 1	382	550	513	4	654
ROI 2	422	590	591	4	683
ROI 3	552	1011	970	2	1056
ROI 4	333	915	874	4	949
ROI 5	400	873	867	16	922
	% cells expressing:				
ROI 1	58,4097859	84,0978593	78,440367	0,6116208	
ROI 2	61,7862372	86,3836018	86,5300146	0,58565154	
ROI 3	52,2727273	95,7386364	91,8560606	0,18939394	
ROI 4	35,089568	96,4172813	92,0969442	0,42149631	
ROI 5	43,3839479	94,6854664	94,0347072	1,73535792	
MEAN	50,1884533	91,464569	88,5916187	0,7087041	
SD	10,9626722	5,77182447	6,32197007	0,59807117	

Patient sample: 29P					
ROIs analysed	5				
	# cells expressing				total # cells
	PSMA	AMACR	AR	KI67	DAPI
ROI 1	706	1217	926	9	1367
ROI 2	479	1449	1296	7	1515
ROI 3	847	1954	1928	8	2250
ROI 4	922	1682	1547	10	1798
ROI 5	818	949	844	11	1072
	% cells expressing:				
ROI 1	51,646	89,027	67,740	0,658	
ROI 2	31,617	95,644	85,545	0,462	
ROI 3	37,644	86,844	85,689	0,356	
ROI 4	51,279	93,548	86,040	0,556	
ROI 5	76,306	88,526	78,731	1,026	
MEAN	49,6985431	90,7179164	80,7488814	0,61165414	
SD	17,222686	3,70608636	7,88528781	0,25739634	

Figure 8.2. Raw data for the image analysis of the primary tumor samples. Each table presents the number of cells expressing each biomarker and the corresponding percentage of biomarker expression, numbers obtained by performing a semi-automated image analysis of ROIs with the QuPath software.

Patient sample: 18M1					
ROIs analysed	5				
	# cells expressing				total # cells
	PSMA	AMACR	AR	KI67	DAPI
ROI 1	812	158	277	3	832
ROI 2	1070	413	537	9	1116
ROI 3	502	176	254	0	514
ROI 4	154	44	78	0	154
ROI 5	754	288	699	5	772
	% cells expressing:				
ROI 1	97,5961538	18,9903846	33,2932692	0,36057692	
ROI 2	95,8781362	37,0071685	48,1182796	0,80645161	
ROI 3	97,6653696	34,2412451	49,4163424	0	
ROI 4	100	28,5714286	50,6493506	0	
ROI 5	97,6683938	37,3056995	90,5440415	0,64766839	
MEAN	97,7616107	31,2231853	54,4042567	0,36293939	
SD	1,4665598	7,68494228	21,3907103	0,36784143	

Patient sample: 18M2					
ROIs analysed	6				
	# cells expressing				total # cells
	PSMA	AMACR	AR	KI67	DAPI
ROI 1	357	369	261	40	397
ROI 2	147	173	105	7	173
ROI 3	142	197	101	28	197
ROI 4	132	191	136	17	202
ROI 5	207	254	130	35	260
ROI 6	72	135	58	36	135
	% cells expressing:				
ROI 1	89,924	92,947	65,743	10,076	
ROI 2	84,971	100	60,694	4,046	
ROI 3	72,081	100	51,269	14,213	
ROI 4	65,347	94,554	67,327	8,416	
ROI 5	79,615	97,692	50,000	13,462	
ROI 6	53,333	100	42,963	26,667	
MEAN	74,212	97,532	56,333	12,813	
SD	13,4973386	3,10437818	9,72558834	7,71997165	

Patient sample: 15M					
ROIs analysed	7				
	# cells expressing				total # cells
	PSMA	AMACR	AR	KI67	DAPI
ROI 1	156	49	171	12	307
ROI 2	41	32	38	5	58
ROI 3	87	133	327	44	426
ROI 4	209	125	125	43	260
ROI 5	85	70	65	15	134
ROI 6	228	127	166	66	493
ROI 7	13	114	164	16	214
	% cells expressing:				
ROI 1	50,8143322	15,9609121	55,7003257	3,90879479	
ROI 2	70,6896552	55,1724138	65,5172414	8,62068966	
ROI 3	20,4225352	31,2206573	76,7605634	10,3286385	
ROI 4	80,3846154	48,0769231	48,0769231	16,5384615	
ROI 5	63,4328358	52,238806	48,5074627	11,1940299	
ROI 6	46,2474645	25,7606491	33,6713996	13,3874239	
ROI 7	6,07476636	53,271028	76,635514	7,47663551	
MEAN	48,2951721	40,2430556	57,83849	10,2078105	
SD	26,8650328	15,6984478	16,0276452	4,09939387	

Patient sample: 22M					
ROIs analysed	5				
	# cells expressing				total # cells
	PSMA	AMACR	AR	KI67	DAPI
ROI 1	0	783	345	1284	2175
ROI 2	0	439	604	478	2033
ROI 3	0	551	1287	403	2306
ROI 4	0	595	2645	421	3099
ROI 5	0	925	2215	526	2949
	% cells expressing:				
ROI 1	0	36	15,862	59,034	
ROI 2	0	21,594	29,710	23,512	
ROI 3	0	23,894	55,811	17,476	
ROI 4	0	19,200	85,350	13,585	
ROI 5	0	31,367	75,110	17,837	
MEAN	0	26,4108399	52,3686211	26,2888531	
SD	0	7,03650247	29,423456	18,6445647	

Patient sample: 27M					
ROIs analysed	9				
	# cells expressing				total # cells
	PSMA	AMACR	AR	KI67	DAPI
ROI 1	0	308	0	297	458
ROI 2	38	266	0	122	306
ROI 3	97	333	0	92	333
ROI 4	5	439	0	208	439
ROI 5	97	561	0	190	561
ROI 6	10	224	0	115	234
ROI 7	43	256	0	126	256
ROI 8	40	263	0	167	263
ROI 9	69	291	0	134	291
	% cells expressing:				
ROI 1	0	67,2489083	0	64,8471616	
ROI 2	12,4183007	86,9281046	0	39,869281	
ROI 3	29,1291291	100	0	27,6276276	
ROI 4	1,13895216	100	0	47,38041	
ROI 5	17,2905526	100	0	33,8680927	
ROI 6	4,27350427	95,7264957	0	49,1452991	
ROI 7	16,796875	100	0	49,21875	
ROI 8	15,2091255	100	0	63,4980989	
ROI 9	23,7113402	100	0	46,04811	
MEAN	13,3297533	94,4337232	0	46,8336479	
SD	9,98613335	11,0844506	0	12,2455007	

Patient sample: 29M					
ROIs analysed	6				
	# cells expressing				total # cells
	PSMA	AMACR	AR	KI67	DAPI
ROI 1	477	477	437	23	477
ROI 2	334	334	289	26	334
ROI 3	796	796	726	14	796
ROI 4	558	558	499	19	558
ROI 5	531	531	431	16	531
ROI 6	281	281	259	8	281
	% cells expressing:				
ROI 1	100	100	91,614	4,822	
ROI 2	100	100	86,527	7,784	
ROI 3	100	100	91,206	1,759	
ROI 4	100	100	89,427	3,405	
ROI 5	100	100	81,168	3,013	
ROI 6	100	100	92,171	2,847	
MEAN	100,000	100,000	88,685	3,938	
SD	0	0	4,21438712	2,12860379	

Figure 8.3. Raw data for the image analysis of the metastatic tumor samples. Each table presents the number of cells expressing each biomarker and the corresponding percentage of biomarker expression, numbers obtained by performing a semi-automated image analysis of ROIs with the QuPath software.

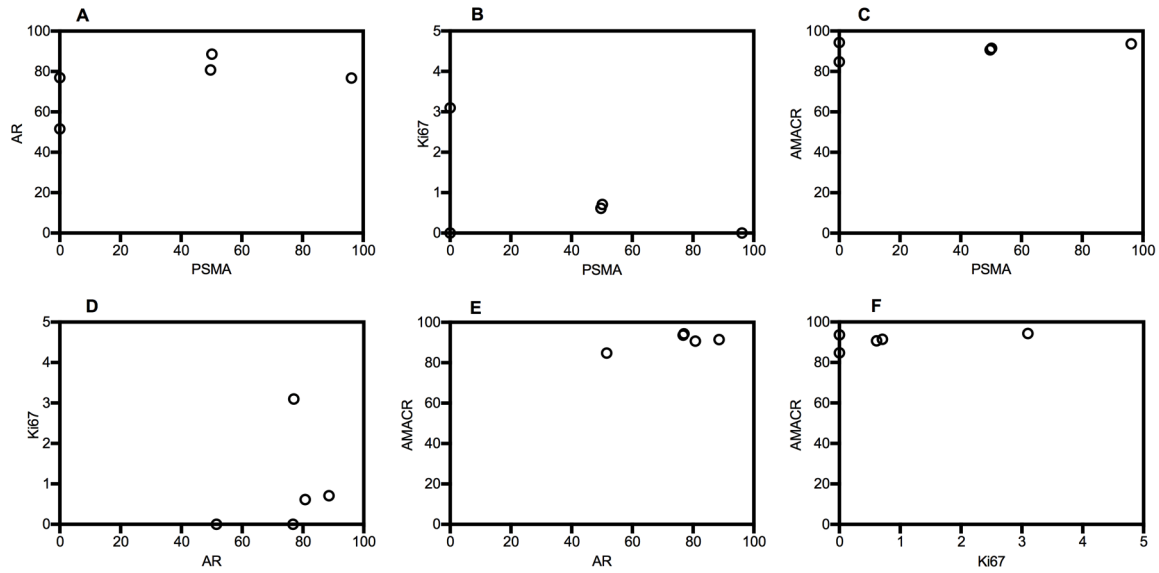

Figure 8.4. Spearman rank correlation for quantitative variables in the primary lesions. There was no significance found in all correlations between the biomarkers expression levels (A-F).

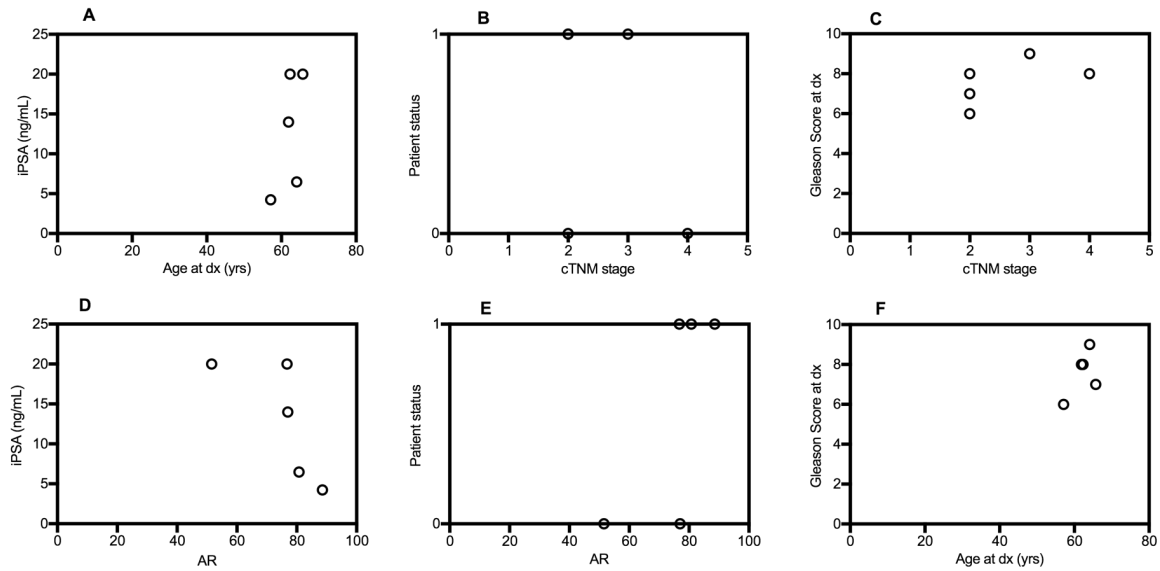

Figure 8.5. Spearman rank correlation of quantitative and qualitative (iPSA, patient status (0 – dead; 1 – alive), cTNM stage, age and Gleason score at dx) variables in the primary lesions. There was no significance found in all correlations between the qualitative variables data (A-C, F). iPSA and AR were negatively correlated (r=-0,9747, p-value=0,0333).

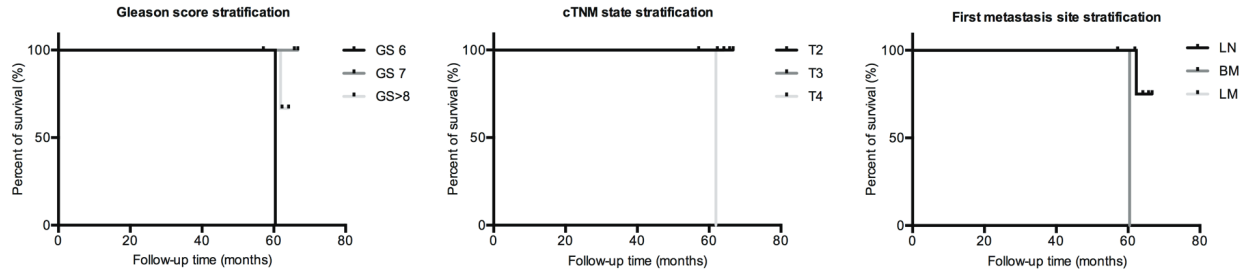

Figure 8.6. Analysis of the influence of clinico-pathological data variables at diagnosis in the patients' survival. Kaplan-Meier curves with all sample data, stratified by the Gleason Score and cTNM state at diagnosis (first two graphs, from left), and by the first metastasis site (right).

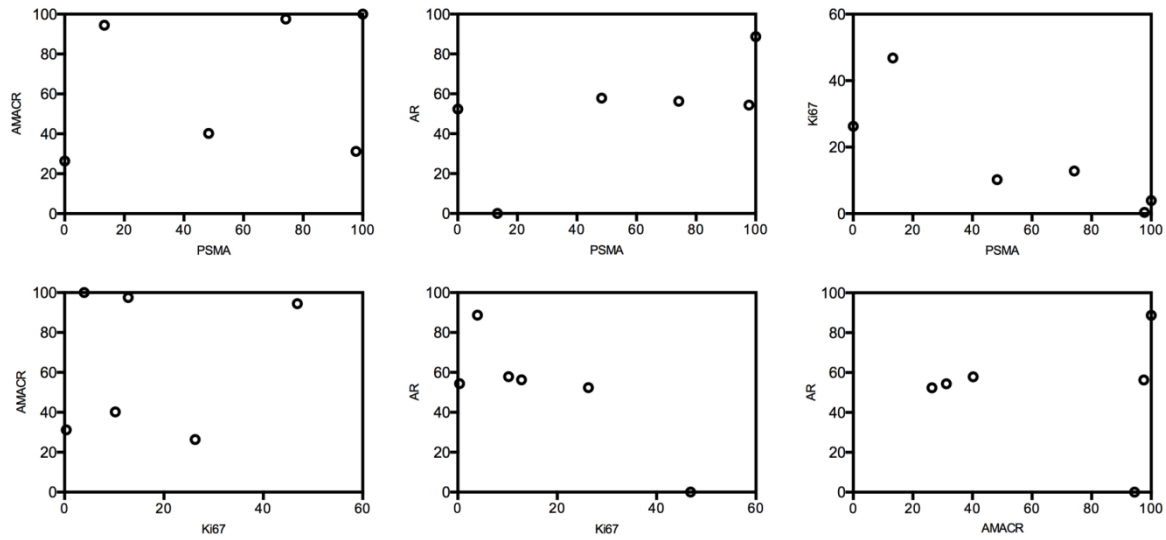

Figure 8.7. Spearman rank correlation for quantitative variables in the metastatic lesions. There was no significance found in all correlations between the biomarkers expression levels.

Table 8.1. Spearman rank correlation using quantitative variables (all biomarkers) for all metastatic lesions (n=6).

	PSMA	*AMACR*	*AR*	*Ki-67*
PSMA				
r	1	0,6	0,7143	-0,8286
p-value		0,2417	0,1361	0,0583
AMACR				
r		1	0,5429	-0,08571
p-value			0,2972	0,9194
AR				
r			1	-0,6571
p-value				0,175
Ki-67				
r				1
p-value				

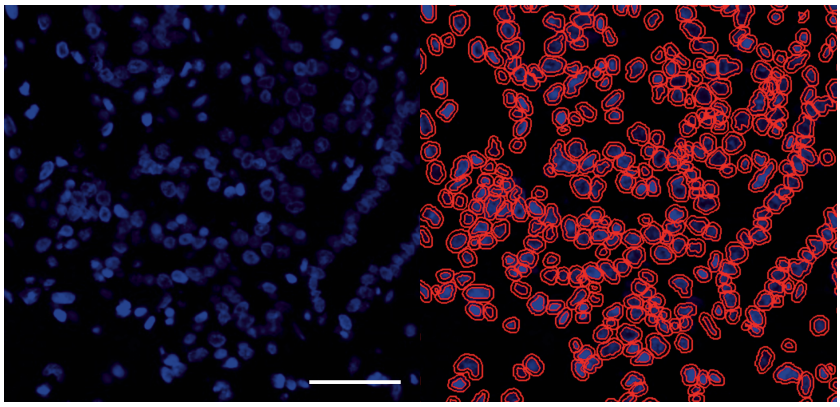

Figure 8.8. Example of the QuPath automated cell detection tool. Scale bar – 100 µm.